PHOTOCATALYTIC CONVERSION OF CO_2 TO HYDROCARBONS USING Cu-Zn/TiO_2 CATALYST

BY

Adeem Ghaffar Rana

A Thesis Presented to the
DEANSHIP OF GRADUATE STUDIES

KING FAHD UNIVERSITY OF PETROLEUM & MINERALS

DHAHRAN, SAUDI ARABIA

In Partial Fulfillment of the
Requirements for the Degree of

MASTER OF SCIENCE

In

CHEMICAL ENGINEERING

May, 2015

KING FAHD UNIVERSITY OF PETROLEUM & MINERALS

DHAHRAN- 31261, SAUDI ARABIA

DEANSHIP OF GRADUATE STUDIES

This thesis, written by **Adeem Ghaffar Rana** under the direction his thesis advisor and approved by his thesis committee, has been presented and accepted by the Dean of Graduate Studies, in partial fulfillment of the requirements for the degree of **MASTER OF SCIENCE IN CHEMICAL ENGINEERING.**

Dr. Ali Al-Matar 28/5/2015
(Advisor)

Dr. Mohammed Ba-Shammakh
Department Chairman

Dr. Reyad A. Shawabkeh
(Member)

Dr. Salam A. Zummo
Dean of Graduate Studies

Dr. Ibnelwaleed Ali Hussein
(Member)

22/6/15
Date

Dr. Abdulhadi Al-Juhani
(Member)

Dr. Nabeel Salim M. Abo-Ghander
(Member)

To My Parents and Family

ACKNOWLEDGMENTS

First of all thanks to Almighty Allah He gave me strength and sound health to pursue my higher education in KFUPM and completing the study on time. My family without their moral support time might not be that easy.

This thesis would not have been possible without the support of many people. I am thankful to my Advisor Dr Ali Al-Matar for this support and encouragement throughout the research work I am gratefully thankful to my Co-Advisor Dr Reyad Shawabkeh without whom support I might not graduate today. I pay my sincere gratitude for his supervision, guidance, encouragement throughout the research work and help in making this possible. I am extremely thankful to my committee members, Dr. Ibnelwaleed Ali Hussein, Dr. Abdulhadi Al-Juhani and Dr. Nabeel Salim M. Abo-Ghander for their valuable comments and recommendation for making this work more fruitful. I am extremely thankful to Mr. Hatim of Research Institute for his help in characterizing the samples.

At the end, special thanks to Chemical Engineering Department of King Fahd university of Petroleum and minerals for awarding me scholarship for the master degree in their esteem institute and facilitation in completing this research. Last but not the least I pay my heartiest gratitude to my friend of Hetero Group (Lala, Naeem, Waqar, Saqib, Fahad and Aamir), Chutzpah Group (Zaheer, Shah ji, Izhar, Qasim), Catalysis Group (Abdullah Musbah) and all Pakistani community for their support and love during my thick and thin of the time.

TABLE OF CONTENTS

LIST OF TABLES

LIST OF FIGURES

ABSTRACT

Full Name : Adeem Ghaffar Rana

Thesis Title : Photocatalytic conversion of CO2 to hydrocarbons using Cu-Zn/TiO2 catalyst

Major Field : Chemical Engineering

Date of Degree : May 2015

From the ten years there is a 5% (20ppm) increase of CO_2 in the atmosphere which is due to the burning of hydrocarbons. Photocatalytic technology is used to recycle this atmospheric CO_2 to valuable hydrocarbons. Reduction of CO_2 to hydrocarbons reduces the CO_2 in the atmosphere as well as partly fulfills the energy requirements of the world in the form of fuel.

In this work the aim is to study the effect of the metal modified titanium dioxide (TiO_2) on the photocatalytic reduction of the carbon dioxide (CO_2). A series of metal modified TiO_2 catalyst was synthesized using the wet impregnation method. The metals chosen for this purpose were Cu and Zn. Cu and Zn modified catalysts were tested for the photocatalytic reduction of CO_2.

The synthesized catalysts were characterized by using different analytical techniques such as powder XRD, SEM, EDX, N_2 adsorption isotherm, FTIR and TGA. It is found that the phase of the metal modified catalyst remains the same i.e. Anatase. The surface area of the metal modified TiO_2 was found to be 8.59 m^2/g. It is confirmed by XRD that Cu and Zn are successfully loaded on the surface of the catalyst. Elemental composition the loaded metal was found by using EDX analysis. Morphology of the synthesized catalyst was studied using the SEM analysis.

The modified catalysts were test under UV light irradiation of 60W using 3 lamps each of 20W intensity and 254 nm wavelengths. Temperature and pressure condition are room temperature and 1 bar respectively. The catalysts were tested for the two molar ratios of H_2 to CO_2 to 4 and 2. The catalysts were irradiated for 30 min before taking the samples for the analysis. Exit gas stream of the reactor was analyzed using GC and it confirms the conversion of CO_2.

Different series of catalyst were tested for the photo reduction of CO_2. Firstly pure TiO_2 was tested for the conversion of CO_2; the conversion reported for the pure TiO_2 is 9.65% at a molar ratio of 4/1. The conversion efficiency of the catalyst increased by 38% after it is modified by Cu metal. Addition of Zn does not affect the conversion of TiO_2 as Zn failed to act as electron trapper on the surface of TiO_2 due to higher conduction band than that of TiO_2. The co-modification of TiO_2 with both Cu and Zn work synergistically and increase the efficiency of the catalyst by 48 % as compared to Pure TiO_2 and 8% as compared to Cu modified catalyst.

This work is done under UV light but it is suggested for future recommendation to work in solar light and use another set of metals to modify the TiO_2, so the conversion efficiency of the process can be increased and to make this process feasible for the industrial use.

ملخص الرسالة

الاسم الكامل:أديب الغفار رزا

عنوان الرسالة: التحليل الضوئي الحفاز لتحويل CO_2 الى هيردوكربونات باستعمال حفاز $Cu-Zn/TiO_2$

التخصص: الهندسة الكيميائية

تاريخ الدرجة العلمية: مايو 2015

منذ عشر سنين هنالك زيادة في ثاني اكسيد الكربون (20ppm) 5% في الهواء الجوي بسبب احتراق الهيدروكربونات. تقنية التحليل الضوئي الحفاز استعملت لتدوير ثاني اكسيد الكربون الجوي الى الهيدروكربونات مفيدة. اختزال ثاني اكسيد الكربون الى الهيدروكربونات يقلل من ثاني اكسيد الكربون في الهواء الجوي وايضا تعويض جزئي لمتطلب الطاقة في العالم في هيئة وقود.

في هذه الاطروحة, نهدف الى دراسة تأثير ثاني أكسيد التيتانيوم المطور بالمعدن على التحليل الضوئي الحفاز لاختزال ثاني اكسيد الكربون. عديد من ثاني أكسيد التيتانيوم المطور بالمعدن قد تم تحضيره باستعمال تقنية التحليل بالتبليل. المعادن المختارة Cu-Zn-Cu/Zn للتحليل الضوئي الحفاز لاختزال ثاني اكسيد الكربون.

الحفاز المحضر قد تم التأكد منه باستعمال XRD-SEM-EDX-FTIR-TGA و ادمصاص وامتزاز النايتروجين. لوحظ أن طور الحفاز المطور بالمعدن ثابتة في اناتيز. مساحة السطح الحفاز المطور بالمعدن $8.59\ m^2/g$. تم التأكد باسخدام XRD النجاح في تحميل Cu وZn . التكوين العنصري للمعادن المحملة على الحفاز وجدت عن طريق EDX. التكوين الهيكلي للحفاز تمت دراسته بواسطة SEM.

الحفاز المطور بالمعدن تم اختباره باستعمال الاشعة فوق البنفسجية 60 W خلال 3 مصابيح كل منها 20 W ذو شدة قدرها 254 nm طول موجي. الحرارة والضغط كانا حرارة الغرفة و1 bar بالترتيب. الحفاز تم دراسته نسب مولية H_2/CO_2 4-2. الحفاز عرض لمدة 30 min قبل التحليل. الغاز الخارج من المفاعل تم تحليله باستعمال GC و الذي أكد تحويل CO_2.

حفازات متعددة تم اختبارها. أولا ثاني أكسيد التيتانيوم خالصا لاختزال ثاني اكسيد الكربون: التحويل حوالي 9.65% نسبة مولية 4/1. كفاءة التحويل ازدادت 38% مع تدعيم بالمعدن Cu. اضافة Zn لم تؤثر حيث فشلت electron trap على سطح ثاني أكسيد التيتانيوم بسبب conduction band. التحسين المزدوج لثاني أكسيد التيتانيوم مع Cu-Zn بالتآزر على تحسين كفاءة الحفاز 48% بالمقارنة مع ثاني أكسيد التيتانيوم الخالص و 8% الحفاز المعدل بـ Cu.

هذا العمل قد تم معرضا للاشعة فوق البنفسجية ويقترح في المستقبل العمل خلال الاشعة الضوئية واستعمال معادن اخرى لتحسين ثاني أكسيد التيتانيوم, لنتمكن من زيادة كفاءة التحويل وامكانية جعلها مربحة في المجال الصناعي.

CHAPTER 1

INTRODUCTION

1.1 Introduction

One of the key environmental issue for humanity is greenhouse effect [1]. Climate's temperature is increasing as it is obvious from increase in ocean's temperature and average global sea level [2]. Carbon dioxide (CO_2), methane (CH_4) and chloro fluoro carbons (cfcs) are the greenhouse gases which are the main cause for global warming [3]. Among the different greenhouse gases highest emitted by the human activities like deforestation or burning of fuel is CO_2 and it has the highest concentration in the environment [4]. The CO_2 emission is projected to increase 50% in future from 2007 to 2030, which in past has increased almost 80% from 1970 to 2004 [2]. Such an escalation in the emission of CO_2 will increase the average global temperature by 6 ºC till the end of this century [5]. The human survival will be at stake if this increase in not kept under control [6]. Exploring effective methods to resolve this issue is the active research area. The main purpose of the research is to bring down the level of greenhouse gases, especially CO_2 to the safe limit.

Gases emitted globally that are the cause of greenhouse effect are show in Figure 1–1

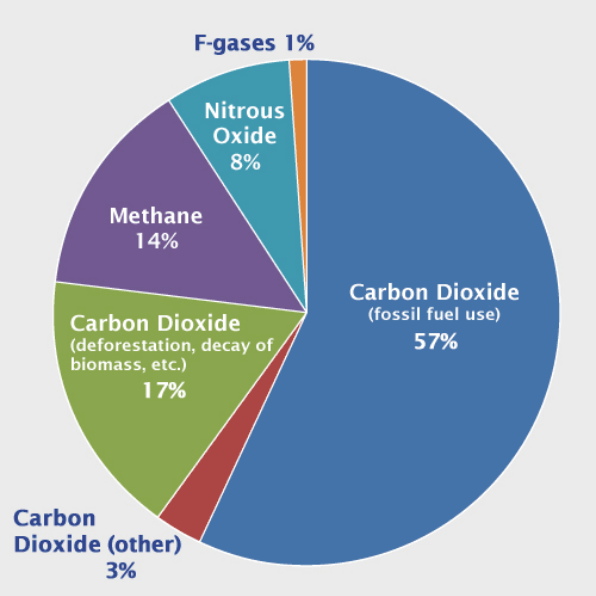

Figure 1–1 Global Gas Emission[7]

These gases are emitted in atmosphere by different sources such as agriculture, forestry, energy supply, transportation and industry in Figure 1–2.

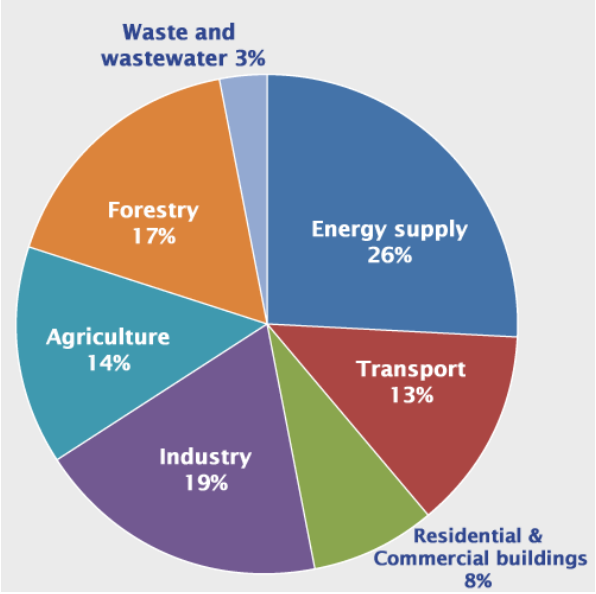

Figure 1–2 Gases Emitted By Sources[7]

Human Development Index (HDI) recognized by United Nations development program as measure of the "Quality of Life". In Figure 1–3 HDI is plotted against energy consumption per capita [8]. It is clear that the countries with better quality of life or HDI index has higher energy consumption e.g. fossil fuels and electricity [9].

CO_2 is a major greenhouse gas and its level must be kept in a safe limit so that it does not affect the world weather. For that purpose many technique are under use like CO_2 capture and utilization processes. Due to the cost and storage factor it is better to utilize CO_2 to make beneficial products rather than capturing. CO_2 can be utilized using different processes like dry reforming, methanol production and hydrogenation of CO_2.

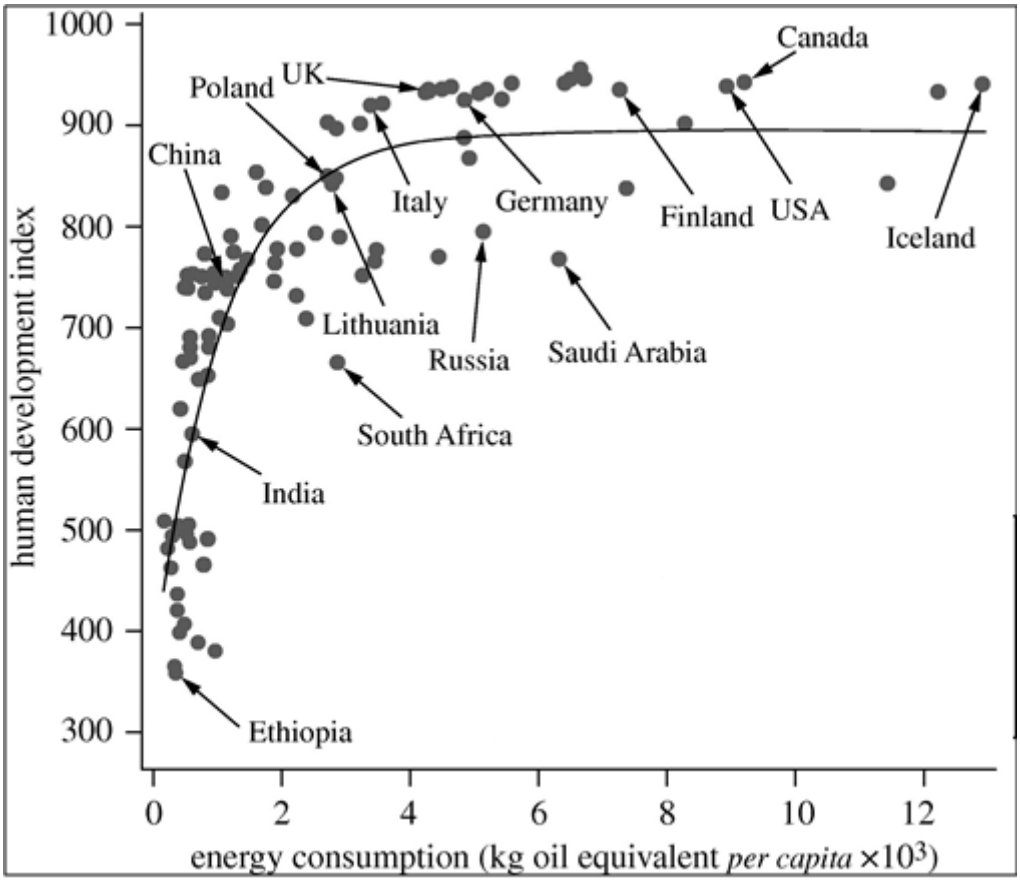

Figure 1–3 Human Development Index of Different Countries [8]

Utilization is a plausible option, because it can lower the CO_2 emission, decrease the consumption of the fuels and can be a course for enough energy for the society [8,10–12]. In Figure 1–4, Gibbs free energy of formation of different materials is shown. The Energy shows that CO_2 is a highly stable molecule. As a result, high energy for the conversion of CO_2 into any fuel is needed [8].

Renewable source of the energy (solar, wind) should be used to avoid further emission of CO_2 while converting CO_2 into fuels. Many techniques can be used e.g. electrochemical conversion of CO_2 into hydrocarbons. H_2 and CO_2 can be reacted directly under suitable conditions to produce methanol [13]. This process of conversion of CO_2 will be efficient if the input energy is produced using renewable energy.

Another technique that can be used of the conversion of CO_2 is the photo reduction with H_2/H_2O by using some semiconductors. The main benefit of this process is that the input energy is light and there will not be any CO_2 emission. Photocatalytic conversion of CO_2 has attracted many researchers in recent decades, but low efficiencies and development of effective catalyst is still the challenge for the researchers.

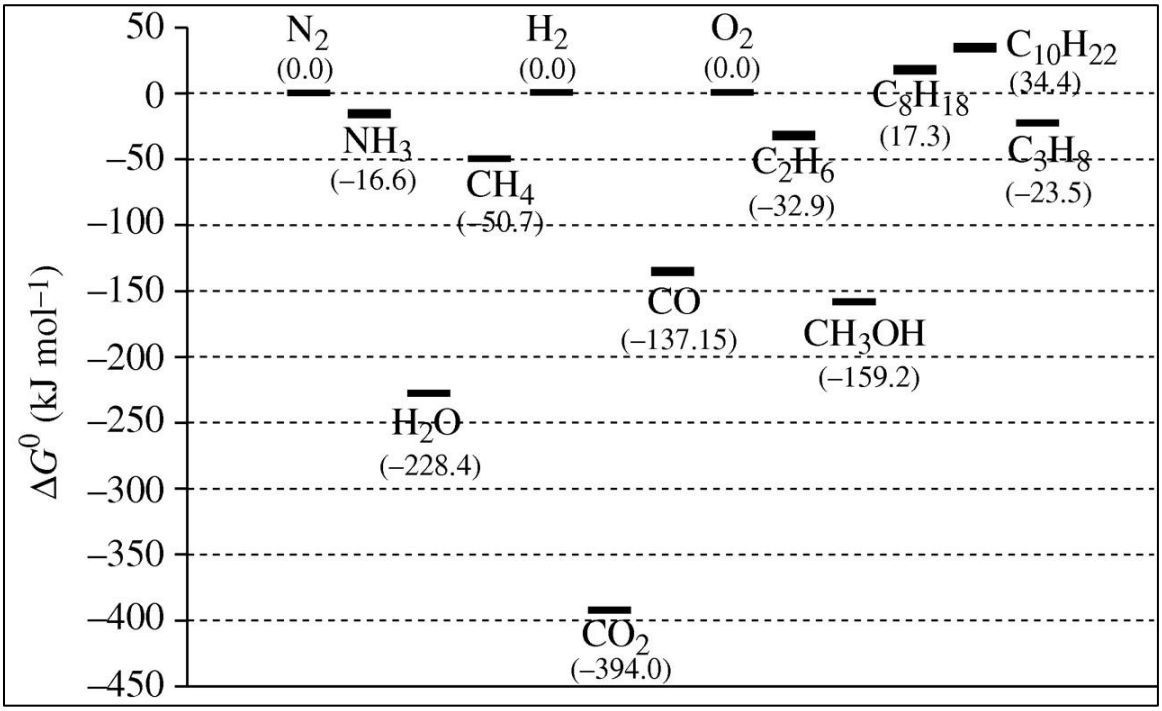

Figure 1–4 Gibbs free energy of the selected Chemicals [8]

Hydrogenation of CO_2 can be done either by chemical catalytic reactions under high temperature and pressure or by photocatalytic reaction under ambient conditions. This work focused on synthesis of effective catalyst and improving the efficiency of the semiconductor photocatalyst for CO_2 photo reduction. Photocatalytic conversion of CO_2 to hydrocarbons is investigated. For that purpose Cu-Zn co impregnated on the surface of TiO_2 is used. To the best of our knowledge, this work is not reported yet in the literature. The further review on CO_2 photo-reduction and detailed objectives of this study are presented ahead.

1.2 Objectives

1. To synthesis of Cu-Zn/TiO_2 based catalyst using impregnation technique.
2. To characterization using XRD, FTIR, BET, TGA, SEM and FTIR
3. To study the photocatalytic conversion of CO_2 into hydrocarbons under UV light irradiation
4. To study the effect of different % of metal loading on the surface of TiO_2

CHAPTER 2

Literature Review

2.1 Carbon Dioxide Sources

2.1.1 Contribution of Man Activities and Natural Sources

The major source of the CO_2 is power plants running by fossil fuels. One third of the CO_2 emitted throughout the world is from these plants. As a general example a coal fired plant of capacity of 1000 MW emits 7 Mt CO_2 per year on the other hand if the plant is fired using oil the CO_2 emission reduces to two third and with natural gas it reduces further to one half. Secondly there are many industrial processes which emit highly concentrated CO_2 streams as byproducts. CO_2 can be captured and stored from the wells from where the natural gas is being extracted. Land use changes are when forest or agricultural lands are converted to human used areas. This affect is causing 3.3 billion tons of CO_2 which makes almost 9% [14] shown in Figure 2–1. Deforestation is the major cause of this problem as trees sink carbon dioxide and remove it from atmosphere by using it via photosynthesis. Due to deforestation, the number of trees in the environment decreases eventually the CO_2 removed by photo synthesis will also reduces. CO_2 is also released in atmosphere by natural process alongside the human activities. Ocean atmosphere exchange contributes 42.84% while animal respiration as well as soil respiration and decomposition produce 28.56% each [15] and volcanoes contribute minor amount 0.03% shown in Figure 2–2.

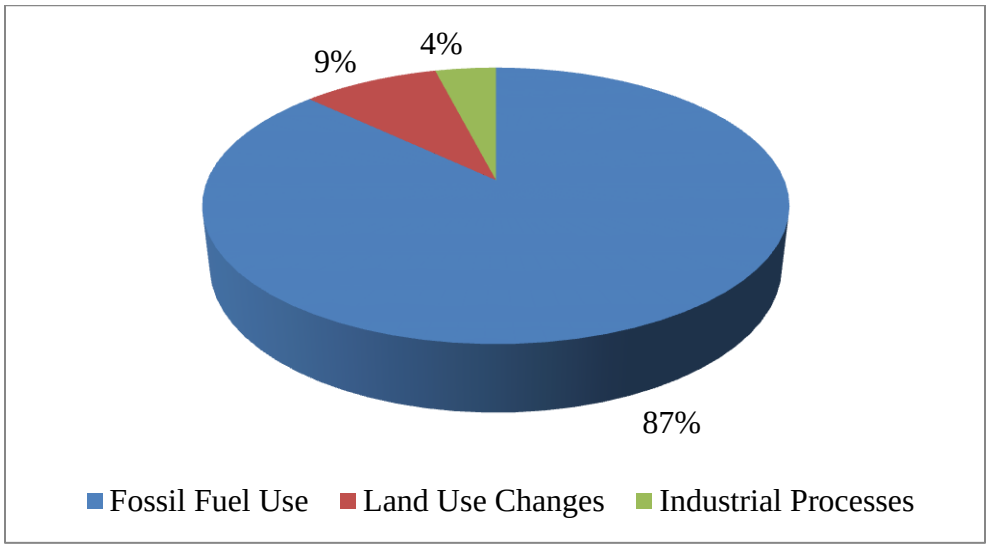

Figure 2–1 Human Sources of CO_2 [14]

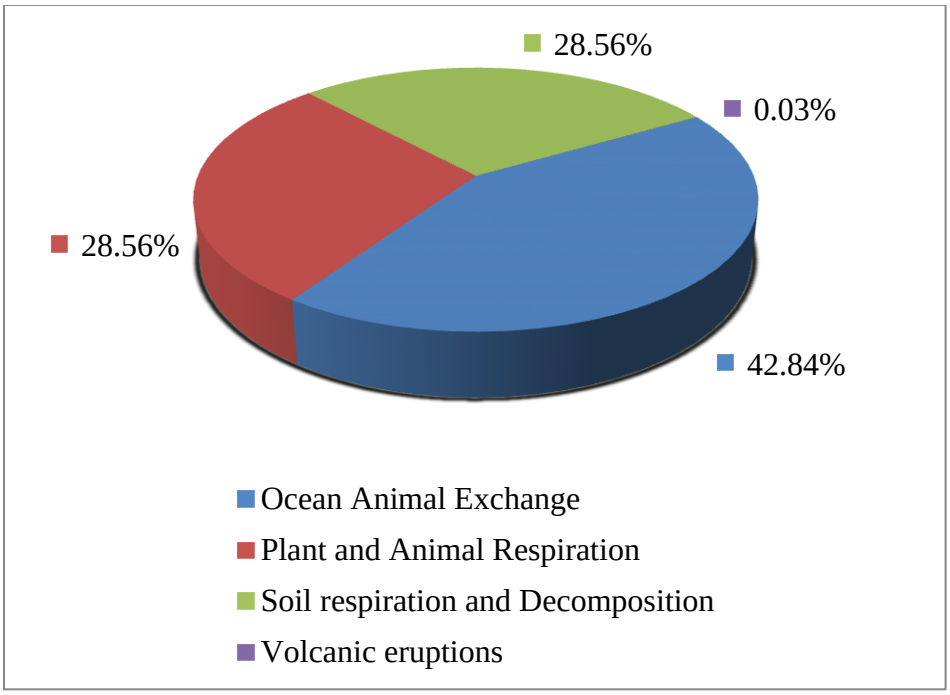

Figure 2–2 Natural Sources of CO_2 [14]

2.2 Carbon Dioxide Sequestration

Carbon sequestration and storage (CSS) is an efficient technique to lower CO_2 level in atmosphere as proposed by many studies. CSS is a technique to capture CO_2 from emission sources and store it in reservoirs of oil, gas and deep sea [1]. One of the drawback of CSS is that it needs additional energy and cost for the transportation, compression, separation, storage and purification [5]. One of the basic reasons of CSS is to allow human beings use of the fossil fuels which is the major portion (almost 86%) of the energy consumed and it is main source of the CO_2 emitted (nearly 75%) by human activities [16]. As a result of reduction of CO_2 in the atmosphere we are making global climate change less severe. CO_2 capture processes are classified to [16]

1. Flue gas separation
2. Oxy-fuel combustion in power plants
3. Pre-combustion separation

Few key points should be kept in mind while storing CO_2 [17]

1. Long storage time
2. Cost should be minimized
3. Safety precautions to avoid any accidents
4. Minimum environmental effect
5. Should abide by all national and international laws

CO_2 is mainly stored and consumed in oil & gas reservoirs, enhanced oil recovery, coal seams and deep saline formations [17].

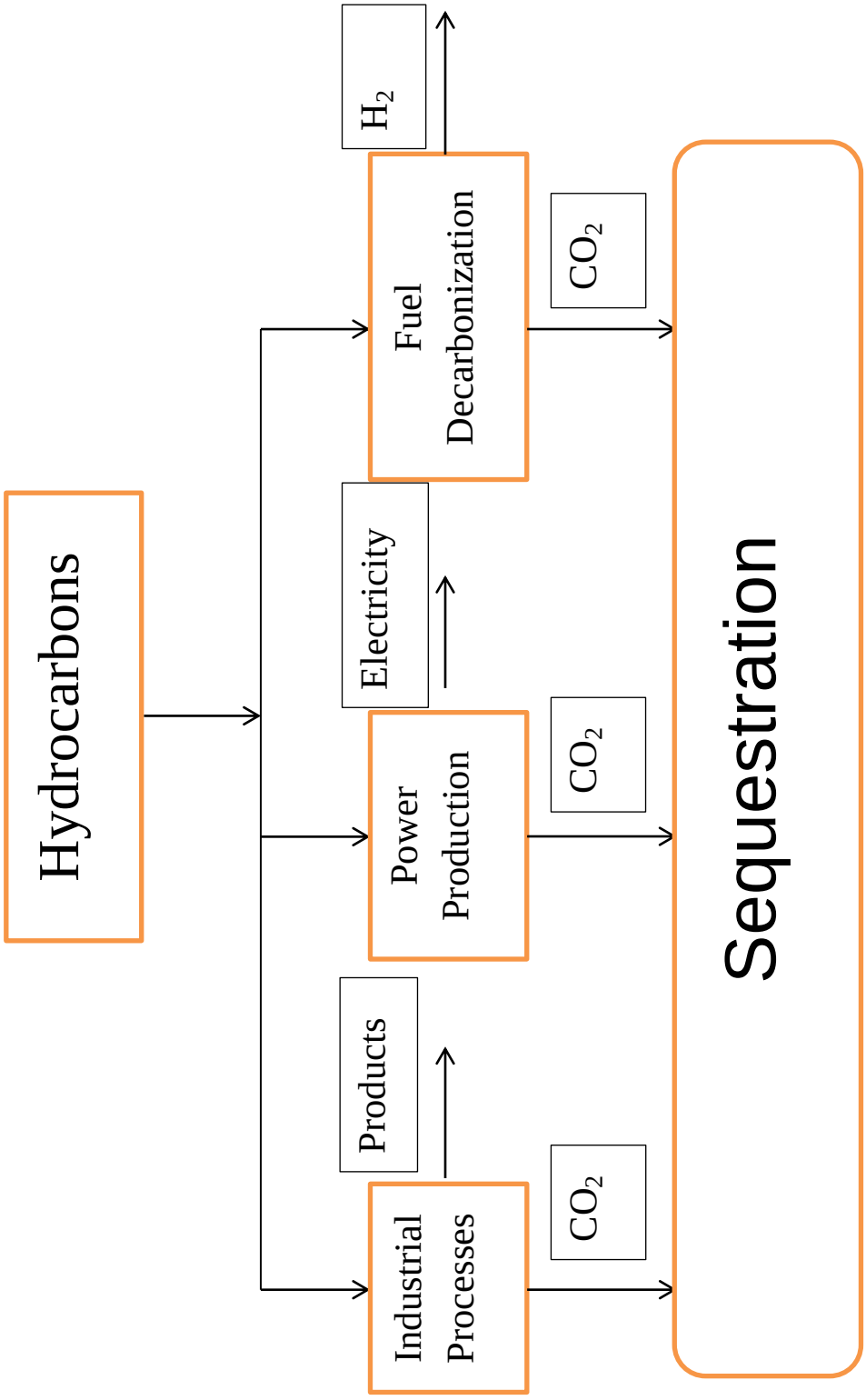

Figure 2–3 Flow Diagrams of CO_2 and Its Sequestration [16]

2.3 Carbon Dioxide Utilization

CO_2 transformation is considered more to be attractive than its storage, if feasible routes are available. These days, conversion of CO_2 to valuable products is getting more attention. There are many processes available from which few are discussed below.

2.3.1 Direct Transformation of CO_2 to Carbonates and Epoxide

Direct transformation of CO_2 over heterogeneous catalysts is one of the methods. From almost last 20 years or so a wide range of catalysts have been used for transformation of CO_2. Transformation of CO_2 to cyclic carbonate, dimethyl carbonate, and epoxide are the few processes used. The catalysts used for this are inorganic metal oxides, clay and zeolite as well as the organic base catalysts [18].

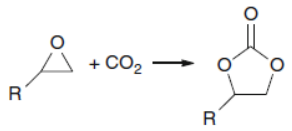

R = H (EO: ethylene oxide, EC: ethylene carbonate)
CH_3 (PO: propylene oxide, PC: propylene carbonate)
C_6H_5 (SO: styrene oxide, SC: styrene carbonate)

2.3.2 CO_2 Utilization for Urea

CO_2 is utilized indirectly in organic synthesis of many valuable chemicals. In industries CO_2 is utilized for the production of methanol, urea, salicylic acid, poly and cyclic carbonates [18]. CO_2 utilized for the production of urea is approximately 100 million tons on industrial scale. Same like urea 90,000, 80,000 and 70,000 tons salicylic acid, cyclic carbonates and poly carbonates are synthesized in industry respectively [18]. Hydrogenation of CO_2 is another process for the utilization of CO_2 and mitigating the greenhouse effect. Conversion of CO_2 to CH_4 and CH_3OH is promising research topic

now a days, but practical industrial process has not been developed yet because of the limitation of reactivity of CO_2, thermodynamic stability and economic feasibility [18].

2.3.3 Synthesis of DMC

CO_2 can be utilized for the production of dimethyl carbonate either by trans-esterification of cyclic carbonate or by direct synthesis from CH_3OH [18].

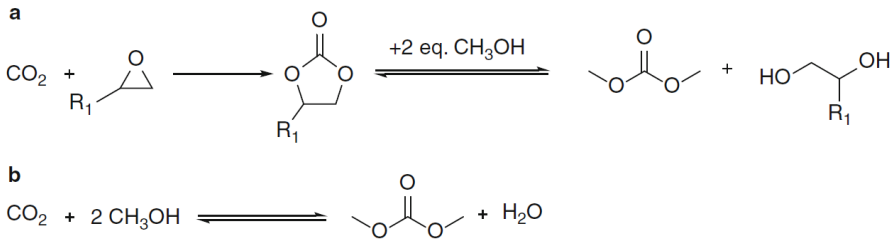

2.3.4 Transformation to Methanol & Di-methyl ether

CO_2 can be utilized for the formation of methanol and dimethyl ether. Di methyl ether and methanol can be alternative to LPG and gasoline. This transformation has major two benefits, first it utilize CO_2 and secondly it can be utilized as fuel instead of oil [18].

$$CO_2 + 3\ H_2 \leftrightarrows CH_3OH + H_2O \qquad \text{(Methanol Synthesis)}$$

$$2\ CO_2 + 6H_2 \leftrightarrows C_2H_6O + 3H_2O \qquad \text{(Di Methyl Ether Synthesis)}$$

2.3.5 Syngas Production or Dry Reforming

CO_2 is utilized for the production of syngas using reforming of CO_2. CH_4 is converted to syngas using dry reforming. Syngas is a mixture of H_2 and CO. Methane reforming is represented by following equation [18]

$$CH_4 + CO_2 \rightarrow 2CO + 2H_2$$

2.4 Methanation of Carbon Dioxide

The main purpose of the CO_2 conversion is to achieve the complete reduction to the methane by homogeneous catalysis.

$$CO_2 + 4\ H_2 \rightarrow CH_4 + 2\ H_2O$$

There are three ways of methanation of carbon dioxide

1) Thermal catalytic conversion
2) Electro catalytic conversion
3) Photocatalytic conversion

2.4.1 Thermal Catalytic Conversion

CO_2 can be transformed into valuable compounds using high energy H_2 and CH_4 on industrial scale. Figure 2–4 [19] shows the conversion routes via H_2 directly result in fuels while CO_2 is converted to syngas using CH_4 which in further step converted to any of the above. Direct conversion using H_2 is economically viable.

CO_2 conversion to CH_4 is industrially very important. CH_4 can be used for many purposes like dry reforming, power generation and it can be utilized as fuel.

Nickel and other noble metal are used as catalyst in the conversion of CO_2. Ru is the best in terms of conversion and selectivity among all metals shown in Table 2-1 [19,20]. As the conversion process is exothermic it is desired to synthesis a catalyst for low temperature which favors the CO_2 conversions. Low temperature helps to overcome the undesired RWGS. 100% yield of is CH_4 is reported by [21] at 453 K using Ru on TiO_2 support. CO_2 is converted oxygenates when reacted with H_2.

CO_2 is converted to hydrocarbons directly using cobalt and iron based catalyst. CO is important reaction intermediate when iron based catalysts are used for CO_2-FT reactions [32, 42, 43].

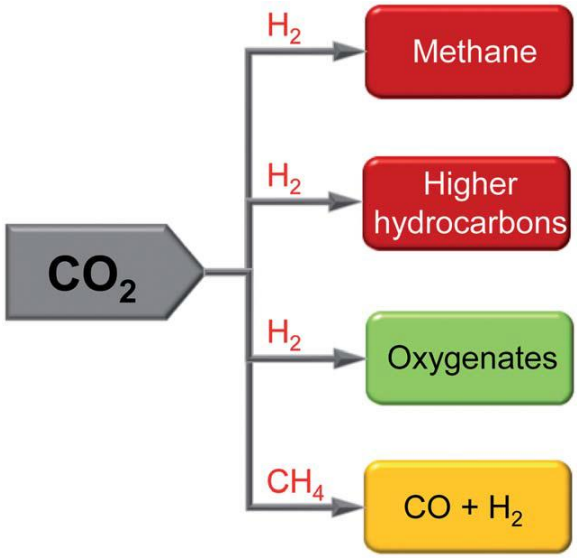

Figure 2–4 CO_2 conversions to fuels or useful commodity chemicals [19]

Table 2-1 Conversion and Selectivity for CO_2 Methanantion [19,20]

Catalyst	***T*/K**	***Conversion* (CO_2)/%**	***Selectivity* (CH_4)/%**	***Reference***
$Ru/TiO_2(B)$	453	100	100	[21]
$Ru/TiO_2(W)$	693	100	100	[21]
$Ru/TiO_2(G)$	513	100	100	[21]
$Ru/TiO_2(B)$	473	100	100	[21]
$Ru/TiO_2(B)$	693	100	100	[21]
$Ru/TiO_2(B)$	513	100	100	[21]
$Ce_{0.97}Ru_{0.03}O_2$	753	51	99	[22]
$Ce_{0.96}Ru_{0.04}O_2$	723	55	99	[22]
$Pd–Mg/SiO_2$	723	59	95	[23]
$Pd–Ni/SiO_2$	723	50.5	89	[23]
10Ni–CZ	623	85	99.5	[24]
Ni-MCM-41	673	56	96	[25]

2.4.2 Electro Catalytic Conversion

There is a long history behind electro catalytic reduction of CO_2, since last few decades it has attracted attention in academic and industry. CO_2 can be converted to various products on the surface of solid electrodes using electrocatalysis. Figure 2–5 shows the cells that are often used for the CO_2 conversions [19]. The cell must also have the facility to chemically analyze the product formed at the electrodes [26]. Figure 2–6 shows that metal electrodes can be categorized by four different categories depending on the reaction type as reported by [26] [27] [28].

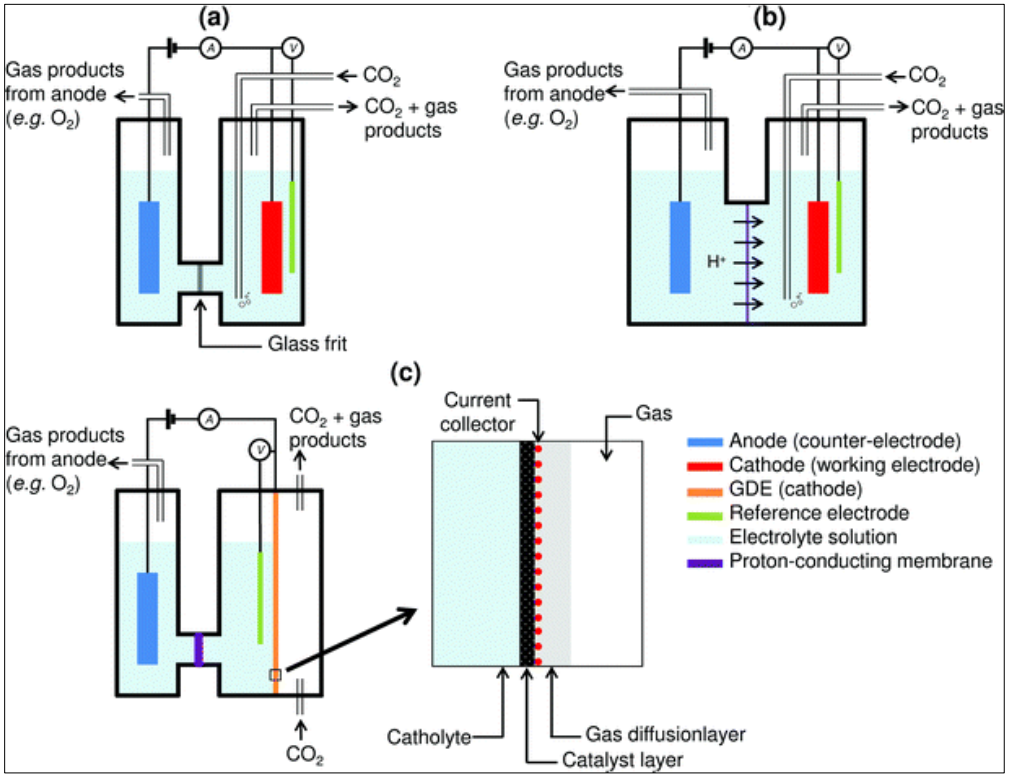

Figure 2–5 Types of Cells used for the Conversion of CO_2 Electrochemically [28]

1. First group contains only copper (Cu) and it shows excellent selectivity and activity for the conversion of CO_2.
2. Second group contains Zn, Au and Ag, the main product for these electrodes is CO.
3. Third group includes Cd, Sn and Pb and these electrodes results in the production of formates as main product.
4. Fourth group metals electrodes produces hydrogen.

The main reason behind hydrogen production is that CO adsorbed inhibits the further reduction of CO_2 [28]. As reported by Hori et.al. [28], many electrodes like C, Al, Mn, Fe, Co, Zr, Nb, Mo, Ru, Hf, Rh Ta, W, Re, V, Si Cr and Ir are mostly inactive for CO_2 reduction at 273 K in a 0.05 M $KHCO_3$ solution performed at -2.2 V standard calomel electrode.

The main challenges still faced by researchers in electrocatalysis are following [19]

1. Requirement of high potential.
2. At room temperature and pressure the solubility of CO_2 is very low.
3. Products formed are in form of mixture and there is additional cost for the separation of these products.
4. Impurities damage the electrodes and cause its deactivation.

The problems are somehow addressed by using Gas Diffusion Electrodes (GDEs). A GDE is mainly Teflon-bonded carbon black matrix on which there are discrete catalyst particles of metals. Firstly it is used by [29] for the Reduction of CO_2. Lead Impregnated GDE is used for the synthesis of Formic acid with current Efficiency of almost 100%.

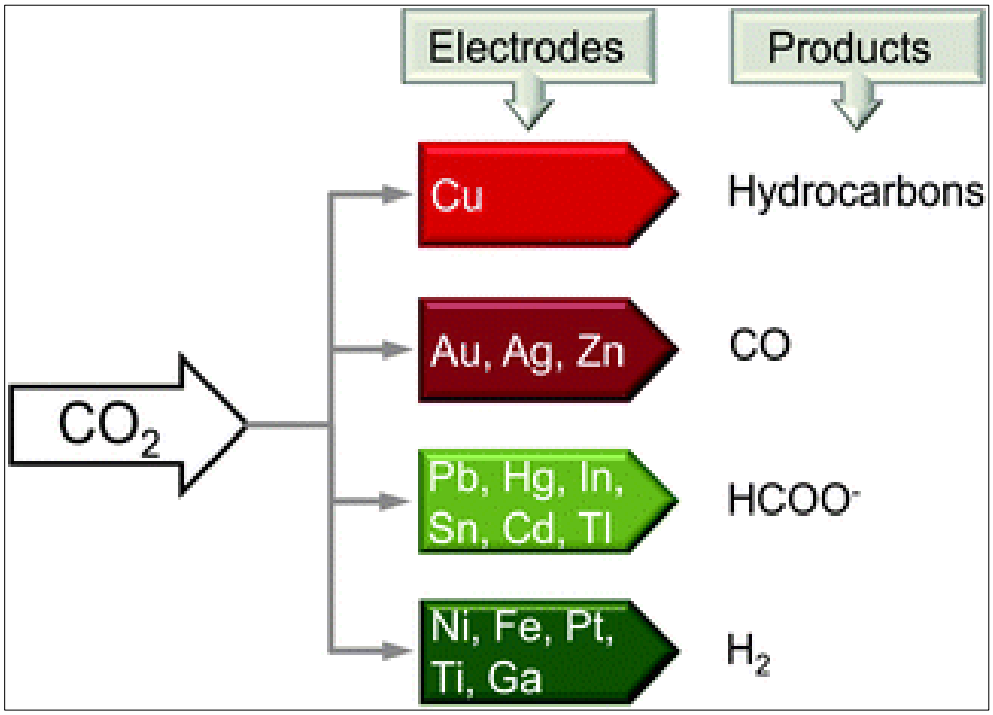

Figure 2–6 Electrode materials and reaction products of CO_2 reduction [28]

2.4.3 Photocatalytic Conversion

Photocatalysis

It is defined as reaction which is being accelerated using a light source and catalyst. The light is adsorbed by the catalyst and electrons moves to an excited state. In this type of reactions, photocatalytic activity of the reaction is determined by the ability to produce and electron hole pair which further produces the hydroxyl radicals, which are used for the main reaction [30].

In conventional catalysis, the process is divided in five steps [31].

1. Bulk diffusion from the fluid to the surface.
2. Adsorption of the reactants on the surface of the catalyst.
3. Reaction on the surface of the catalyst.
4. After the reaction desorption of the products
5. Products formed need to be removed from the interfacial region.

The main difference from chemical catalysis is that in this the activation of catalyst is done through light instead of the thermal source [31].

When a metal oxide or semiconductor is exposed to photons of light which has equal or greater energy than their band bap, the photons get absorbed and create electron hole pairs. It produces photo electrons in the conduction band and photo holes in the valence band. This is shown in the Figure 2–7 schematically [31]. The electron gains energy from photons and move from valence band to the conduction band. While production a +ve charge hole in the valence band and a –ve charge electron in the conduction band [32].

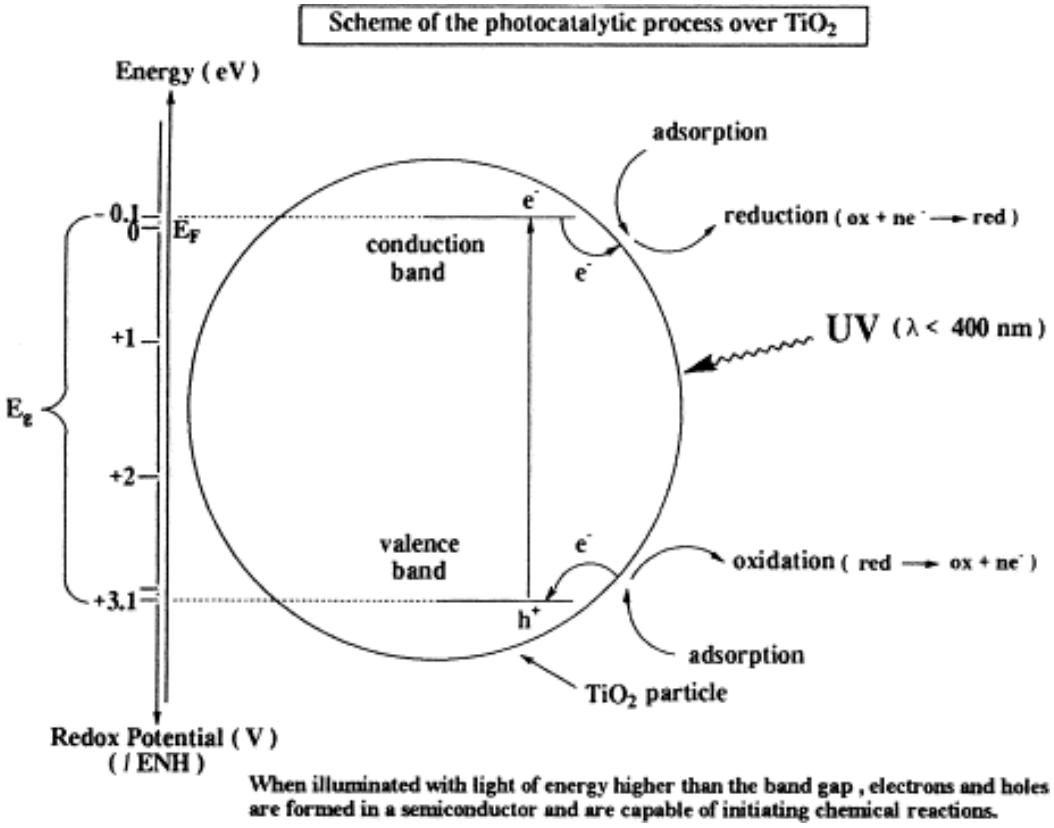

Figure 2–7 Photocatalytic Process Over TiO_2 [32]

Band Gap

The energy gap present between the valence and conduction band of the material is called the band gap. Materials that have high band gaps are called insulators and which have low band gaps are called metals. Metals exhibits insulator property at absolute zero but when photons of energy excite these it allow electrons in the conduction band [33]. The Figure 2–8 shows it graphically.

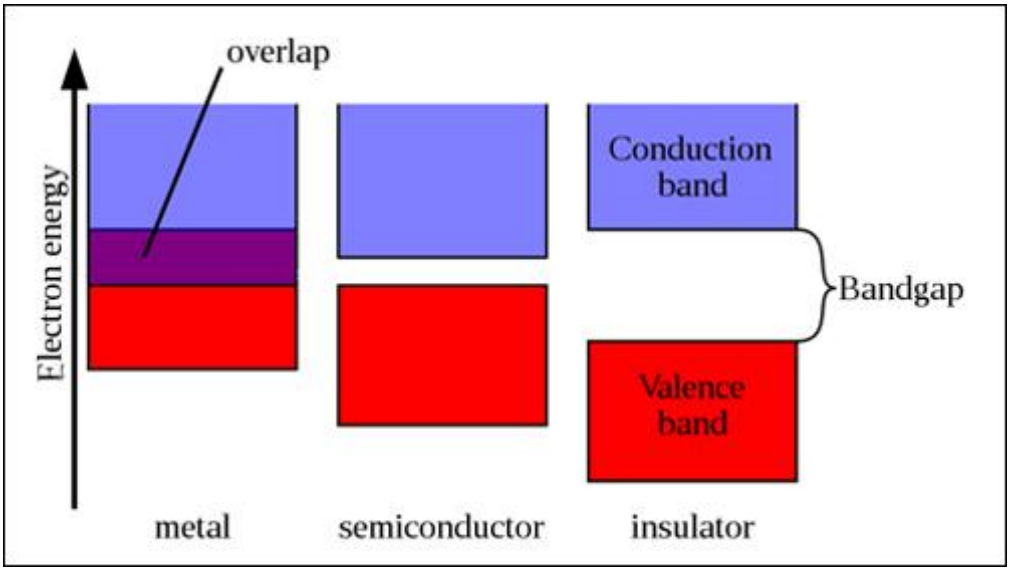

Figure 2–8 Band gap of Different Materials [33]

The band gaps of the different semiconductors are given below in Table 2-2

Table 2-2 Band gaps of Different Semiconductors [34]

Name	**Formula**	**Eg (eV)**	**λ (nm)**	**Range**
Silicon	Si	1.1	1125	IR
Tungsten selenide	WSe_2	1.4	1032	
Copper (II) oxide	CuO	1.35	1032	
Copper (I) oxide	Cu_2O	1.9	620	VIS
Cadmium selenide quantum dots	CdSe QDs	2.0	620	
Ferric oxide (α-phase)/Hematite	α-$Fe2O_3$	2.2	560	
Bismuth vanadate	$BiVO_4$	2.4	517	
Cadmium sulfide	CdS	2.4	517	
Tungsten oxide	WO_3	2.5-2.8	495-442	
Indium tantalum oxide	$InTaO_4$	2.6	477	
Vanadium pentoxide	V_2O_5	2.7	458	
Indium oxide	In_2O_3	2.9	428	
Silicon carbide	SiC	3.0	415	
Titanium oxide (Rutile)	TiO_2	3.02	410	
Titanium oxide (anatase)	TiO_2	3.23	384	UV
Zinc oxide	ZnO	3.2	387	
Strontium titanate	$SrTiO_3$	3.4	364	
Tin dioxide	SnO_2	3.5	354	
Manganese (II) oxide	MnO	3.6	345	
Zinc sulfide	ZnS	3.7	335	
Nickel oxide	NiO	4.3	288	
Aluminum oxide	Al_2O_3	7.1	175	
Magnesium oxide	MgO	7.3	159	

2.5 CO_2 Reduction Reaction Mechanism

Photo reduction of CO_2 consists of complex reaction steps. Firstly the catalyst is excited using light source whose photons should have energy equal or greater than the band gap of the catalyst to move them from the valance band to the conduction band. The excitation causes the production of holes in the valence band and electrons in the conduction band, which helps in photo oxidation and photo reduction. [34]

The energy of the electron of the catalyst should be higher than CO_2 reduction potential. It suggests that the conduction potential of the catalyst have to be above reduction potential of the desired product. At the same time the valence potential of the catalyst have to be below that. Energy level of different products of the system of CO_2 photo reduction reported by Inoue et al. [35] is shown in Figure 2–9

The reaction mechanism starts with the generation of e^- and h^+ pairs. The recombination of the pair to produce heat is the main limiting step in the high efficiency of the reaction as the order of magnitude is higher than the electron transfer [36]. A proposed reaction scheme is shown below reported by many authors [35][36][37].

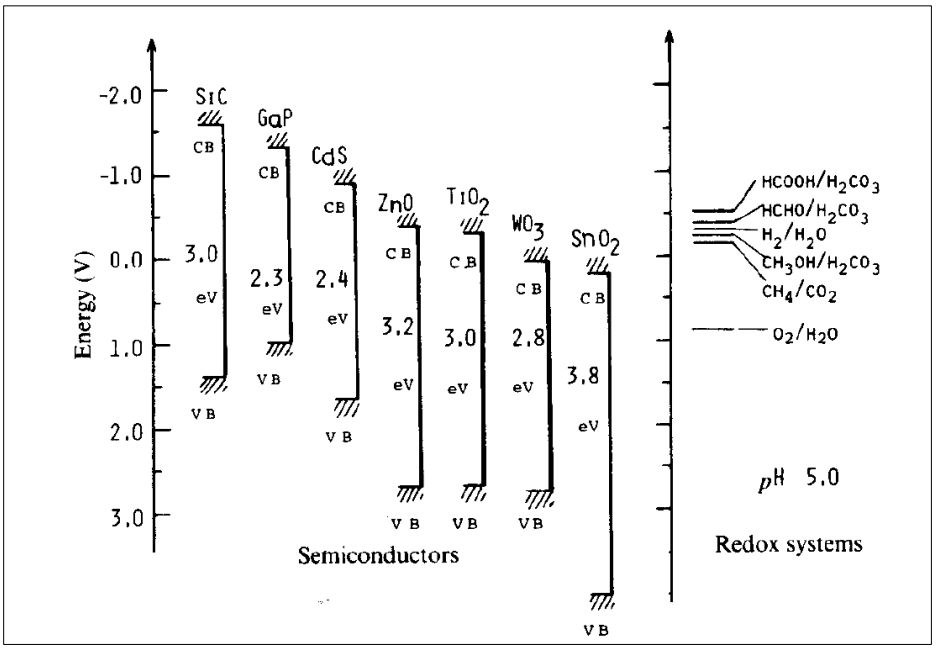

Figure 2–9 Band Gap Energy of Different Semiconductors [35]

Table 2-3 CO_2 Reaction Mechanism

Reaction Step	**Reaction**	**E°**
Initiation Reactions	$Photocatalyst + hv \rightarrow e^- + h^+$	
	$e^- + h^+ \rightarrow heat\ (recombination)$	
Photo Oxidation Reactions	$H_2 + h^+ \rightarrow 2H^+$	
	Photo Reduction Reactions	
Hydrogen formation	$2H^+ + e^- \rightarrow H_2$	$E^o_{redox} = -0.41$
CO_2 Radical Formation	$CO_2 + e^- \rightarrow CO_2^-$	$E^o_{redox} = -1.90$
Formic Acid Formation	$CO_2 + 2H^+ + 2e^- \rightarrow HCO_2H$	$E^o_{redox} = -0.61$
Carbon monoxide Formation	$CO_2 + 2H^+ + 2e^- \rightarrow CO + H_2O$	$E^o_{redox} = -0.53$
Formaldehyde Formation	$CO_2 + 4H^+ + 4e^- \rightarrow HCHO + H_2O$	$E^o_{redox} = -0.48$
Methanol formation	$CO_2 + 6H^+ + 6e^- \rightarrow CH_3OH + H_2O$	$E^o_{redox} = -0.38$
Ethanol Formation	$CO_2 + 12H^+ + 12e^- \rightarrow C_2H_5OH + 3H_2O$	$E^o_{redox} = -0.16$
Methane Formation	$CO_2 + 8H^+ + 8e^- \rightarrow CH_4 + 2H_2O$	$E^o_{redox} = -0.24$

Table 2-4 Year Wise Literature Review

Year	Catalyst	Primary Products	Product Yield		Light Source	Reference
			CH_4	CH_3OH		
1978	GaP ; TiO_2	HCHO, HCOOH, CH_3OH	-	1.88 µmol/h	Hg Lamp	[38]
1979	SiC	HCHO, CH_3OH	-	76.4 (µmol/g-cat/h)	500 WXe/Hg Lamp	[39]
	TiO_2		-	4.86 (µmol/g-cat/h)		
	GaP		-	15.7 (µmol/g-cat/h)		
	CdS		-	16.7 (µmol/g-cat/h)		
	WO_3		-	0 (µmol/g-cat/h)		
1987	Ru/TiO_2	CH_4	105 (µmol/g-cat/h)	-	Solar Simulator	[40]
1992	TiO_2+Cu	HCHO, HCOOH, CH_3OH	-	1.32 (µmol/g-cat/h)	500 W Xe Lamp	[41]
1993	Degussa TiO_2	CH_4, C_2H_6, CH_3OH, HCOOH, CH_3COOH	0.93(µmol/g-cat/h)	-	500 W Hg Lamp	[42]
	Pd-TiO_2		32.93 (µmol/g-cat/h)	-		
	Rh-TiO_2		13.33 (µmol/g-cat/h)	-		
	Pt-TiO_2		6.67 (µmol/g-cat/h)	-		
	Au-TiO_2		4.4 (µmol/g-cat/h)	-		

	$Cu\text{-}TiO_2$		2.53 (µmol/g-cat/h)	-		
	$Ru\text{-}TiO_2$		0.8 (µmol/g-cat/h)	-		
1995	TiO_2 (100)	CH_4, CH_3OH	3.5 (µmol/g-cat/h)	2.4 (µmol/g-cat/h)	75 W Hg Lamp	[43]
	Ti-ZSM-5	CH_4, CH_3Oh, CO	0.17 (µmol/g-cat)	-	75 W Hg Lamp	[44]
	Degussa TiO_2	CH_4, CO, H_2	2 (µmol/g-cat)	-	1000 W Hg Lamp	[45]
1997	TiO_2 (Anatase)	CH_4, C_nH_m	4.74 (µmol/g-cat/h)	-	200 W Hg/Xe Lamp	[46]
1998	Degussa TiO_2	CH_4, HCOOH	0.43(µmol/g-cat/h)	-	4200 W Xe Lamp	[47]
	Pt-Ti/MCM-48	CH_4, CH_3OH	12.3 (µmol/g-cat/h)	0.2 (µmol/g-cat/h)	Hg Lamp	[48]
	Ti-MCM-45		7.6 (µmol/g-cat/h)	3(µmol/g-cat/h)		
1999	$TiO_2/Pd/SiO_2$	CH_4, CH_3OH, HCHO,HCOOH	0.8 (µmol/h)	2.5 (µmol/h)	250 mW Hg Lamp	[49]
	$Li\text{-}TiO_2/Al_2O_3$		2.5 (µmol/h)	0.8 (µmol/h)		
2001	Ti-Beta (OH)	CH_4, CH_3OH	5.76 (µmol/g-cat/h)	1.35 (µmol/g-cat/h)	75 W Hg Lamp	[50]
2002	Cu/TiO_2	CH_3OH	-	19.7 (µmol/g-cat/h)	8 W Hg Lamp	[51]
	Ti-PS film	CH_4, CH_3OH	7.1 (µmol/g-cat/h)	1.8 (µmol/g-cat/h)	1000 W Hg Lamp	[52]
2003	Fe-Cu-K/DAY & $Pt/K_2Ti_6O_{10}$	CH_4,CH_3OH, HCOOH, H_2	0.05(µmol/g-cat/h)	-	150 W Hg Lamp	[53]

2004	TiO_2 (Anatase)	CH_4	0.88(µmol/g-cat/h)	-	UV lamp	[54]
	Cu/TiO_2	CH_3OH	-	23.3(µmol/g-cat/h)	UV Lamp	[55]
	Ag/TiO_2	CH_3OH	-	14.3(µmol/g-cat/h)	8 W Hg Lamp	[56]
	TiO_2/Nafion Film	CH_3OH	-	56(µmol/g-cat/h)	990 W Xe arc Lamp	[57]
	P-25 (1g TiO_2/L Sol)	CH_3OH	-	93.8(µmol/g-cat/h)	15 W UV Lamp	[58]
2005	Cu/TiO_2	CH_3OH	-	0.42(µmol/g-cat/h)	Hg Lamp	[59]
2006	Ru/TiO_2	CH_4, CH_3OH	205 (µmol/g-cat)	13.8 (µmol/g-cat)	1000 W Hg Lamp	[60]
	TiO_2/SiO_2		267.7 (µmol/g-cat)	80.7 (µmol/g-cat)		
	Ru-TiO_2/SiO_2		223.8 (µmol/g-cat)	43.8 (µmol/g-cat)		
2007	MWCNT	CH_4,HCOOH	0.98 (µmol/g-cat/h)	-	15 W UV Lamp	[61]
	TiO_2-MWCNT		11.74 (µmol/g-cat/h)	-		
	TiO_2-Activated Carbon		4.31 (µmol/g-cat/h)	-		
	$CoPc/TiO_2$	CH_4, CH_3OH	0.63(µmol/g-cat/h)	0.21 (µmol/g-cat/h)	500 W Halogen Lamp	[62]

	$InTaO_4$	CH_3OH		1.06(µmol/g-cat/h)	500 W Halogen Lamp	[63]
	$NiO-InTaO_4$			1.39(µmol/g-cat/h)		
2008	TiO_2 (Anatase)	CH_4	33.68 (µmol/g-cat/h)	-	450 W Hg Lamp	[64]
	$Cu-Fe/TiO_2$	CH_4, C_2H_6	0.91 (µmol/g-cat/h)	-	UV Lamp	[65]
2009	Pt-600/NT (N_2 Doped TiO_2 Tubes)	CH_4, CO, Olefins	2.86 (µmol/g-cat/h)	-	Sun Light	[66]
	Cu-600/NT (N_2 Doped TiO_2 Tubes)		3.09 (µmol/g-cat/h)	-		
	TiO_2/SBA-15	CH_3OH	-	972 (µmol/g-cat/h)	400 W Halide Lamp	[67]
	Cu/TiO_2/SBA-15		-	1444 (µmol/g-cat/h)		
	Pt/TO-NT	CH_4	0.13 (µmol/g-cat/h)	-	300W Hg Lamp	[68]
2010	$NiO/InaO_4$	CH_3OH	-	21 (µmol/g-cat/h)	Halogen Lamp	[69]
	Ag/TiO_2	CH_4, CH_3OH	8.5(µmol/g-cat/h)	1.9 (µmol/g-cat/h)	8 W Hg Lamp	[70]
	Cu/TiO_2-SiO_2	CH_4, CO	13.2 (µmol/g-cat/h)	-	Xe arc Lamp	[71]

	Ga_2SO_3	CO	0.72 (μmol/g-cat/h)	-	200 W Hg/Xe Lamp	[72]
	MgO		0.71(μmol/g-cat/h)	-		
	CaO		0.35(μmol/g-cat/h)	-		
	ZrO_2		0.12 (μmol/g-cat/h)	-		
	$ZnGa_2O_4$	CH_4	5.3 (ppm/h)	-	300 W Xe Lamp	[73]
	$RuO_2/ZnGa_2O_4$		50.4 (ppm/h)	-		
	RuO_2+Pt/Zn_2GeO_4	CH_4	25 (μmol/g-cat/h)	-	300 W Xe Lamp	[74]
	CdSe/Pt/TiO_2	CH_4,CH_3OH	0.6 (μmol/g-cat/h)	-	300 W Xe Lamp	[75]
2011	Ti-SBA-15	CH_4,C_2H_4,C_2H_6	0.016 (μmol/g-cat/h)	-	120 W Hg Lamp	[76]
	Kaolinite/TiO_2	CH_4,CH_3OH	0.31(μmol/g-cat/h)	0.18 (μmol/g-cat/h)	8 W Hg Lamp	[77]
2012	TiO_2-RMA	CH_4	2.36 (μmol/g-cat/h)	-	300 W Xe Lamp	[78]
2013	Pt/$CuGaAlO_4$	CH_3OH	-	7.8 (μmol/g-cat/h)	300 W Xe Lamp	[79]
	Mes-CeTi-1.0	CH_4	2220 (μmol/g-cat/h)	-	300 W Xe Lamp	[80]

2.6 Analytical Techniques

2.6.1 Nitrogen (N_2) Adsorption isotherms

Surface area and the pore size distribution of the solid particles is mainly investigated by N_2 adsorption isotherm [81].Sing et.al [81] defined adsorption isotherm as "the relation, at constant temperature, between the amount adsorbed and the equilibrium pressure of the gas". Surface Properties of the sample are investigated and studies using this method. Firstly the sample is outgassed under high vacuum to take out the previously adsorbed sample. After that N_2 is introduced and allowed to adsorb on the sample, N_2 and related pressure are measure at boiling point of N_2. Isotherm is obtained at the end of this measurement [81].

There are six different types of isotherms as shown in the figure below. These isotherms show different properties of the materials as shown and summarized by [82] [81]. For example, there is hysteresis loop in type IV and V which shows the adsorption on mesoporous particle due to multilayer adsorption after that capillary condensation [82]

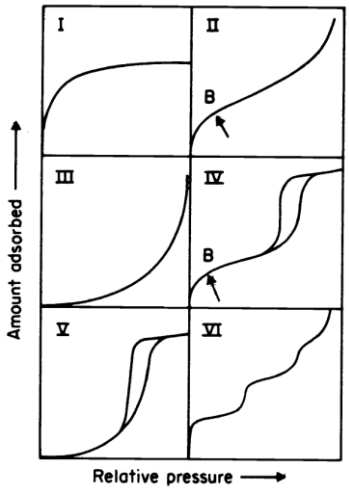

Figure 2–10 N_2 Adsorptiom Isotherms [81]

Surface area of the sample is determined using Brunauer-Emmett-Teller (BET) theory [83] calculating the monolayer capacity of the sample. The equation used for this is shown below.

$$\frac{P}{V\,(P_0 - P)} = \frac{1}{V_m\,C} + \frac{C-1}{V_m\,C}\,(\frac{P}{P_0})$$

where

V = volume of the N_2 adsorbed

V_m = Monolayer capacity

P = Actual N_2 pressure

P_0= Saturation pressure of N_2

C= Constant related to Enthalpy of adsorption

Total and specific surface area is calculated using the equation below with the help of monolayer capacity of the samples.

$$A_S = V_m\,L\,a_m$$

$$a_s = \frac{A_s}{m}$$

where

As= Total surface area

a_s= specific surface area

L=Avogadro constant

a_m= molecular cross-sectional are of N_2

N_2 adsorption isotherms is used to measure the surface area of many materials e.g. TiO_2. Surface area affects the activity of TiO_2. Surface area of Degussa reported by [84] measured by N_2 isotherm is 49 m^2/g. It has been reported by [85] that if the surface area of the material increases the activity of the material increases. Increasing the surface areas will increase the active sites and eventually more species will adsorb on the surface of the material [86].

2.6.2 Powder X-ray diffraction (powder XRD)

Max von Laue in 1912 and W. L. Bragg and W. H. Bragg in 1913 discovered the X-Ray diffraction of the crystals. X-ray diffraction technique is growing since then. One of the major achievements is powder XRD technique. Debye and Scherrer in 1916 first observed in LiF powder and suggested its crystal structure precisely. After that Hull in 1919 and Hanawalt in 1938 formalized a method to determine the crystalline structures of the powder materials [87].

XRD analysis is done by targeting the atoms of the material with X-ray beams. When the X-ray beam hits the electrons of the atoms then it vibrates and re-emit the diffracted rays [88]. A diffraction pattern is formed when these diffracted rays interfere with each other. This type of the pattern is used for the investigation of the atomic structure of the materials [89]. Figure below shows the paths of X-rays through the planes. The angle of

the incident rays is θ, the wavelength of the incident rays is λ and the spacing between the planes is d. according to the Bragg's law [87], there will be constructive interference if the difference in lengths of paths 2dsinθ is equal to the n time wavelength of the incident X-ray, It is expressed mathematically as follow.

$$n\,\lambda = 2\,d\,sin\theta$$

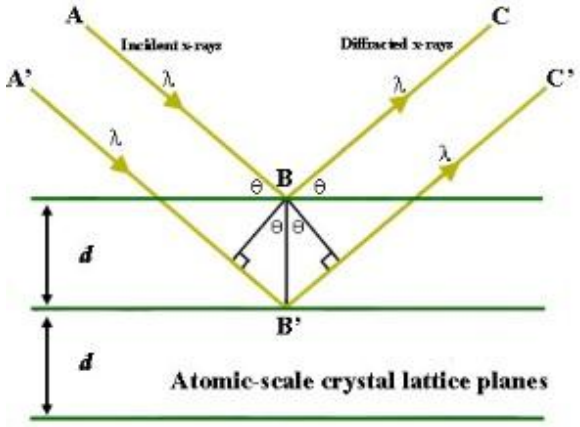

Figure 2–11 X-Rays through the planes [87]

Scanning of crystals with regular planes with fixed wavelength gives characteristic peaks at certain angles, which leads to the mapping of the structure of the crystal of the material. Therefore, the diffraction patterns are presented as intensity versus incident angle [87]. This technique is also used for the study of the structures of TiO_2 as well as if there is any metal loaded or doped on the TiO_2 surface. Lattice spacing changes when there is metal loaded on the surface of the TiO_2. The change can be uniform or non-uniform. In uniform change there is only shift in the peak and for non-uniform there is peak broadening observed [88]. For example, Analysis of Ag doped TiO_2 is shown in

figure below. It shows non-uniform change as there is shift in peak as well as broadening of peak [90].

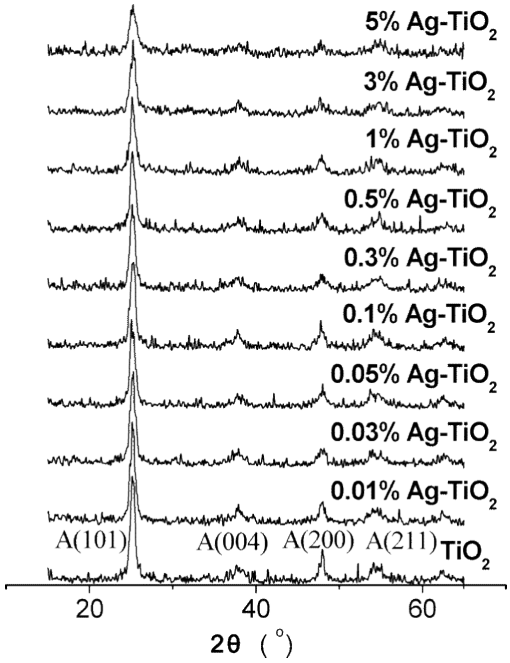

Figure 2–12 XRD of Ag doped TiO_2 [90]

Table 2-5 XRD Shift of Different Doping Ratios of Ag−TiO_2 [90]

Ag doping ratio (mol %)	0	0.01	0.05	0.5	3
2θ (deg)	25.36	25.32	25.26	25.2	25.06

Scherrer formula is used for the calculation of average crystalline size of the material using XRD Data.

$$D = \frac{k\,\lambda}{\beta\,cos\theta}$$

Where [88]

D= Average diameter of crystalline

K=constant ranges in 0.8-1.39

λ= wavelength of the incident X-ray

β= full width at half maximum (FWHM, in radians)

θ= Position of the peak

Following materials and equipment are used in the course of the reaction

2.6.3 Scanning Electron Microscope

Electron microscopy generated from optical microscopy in 1931 when it resolution limit reaches 180 nm due to light diffraction. A high resolution image is generated as a result of small wavelength of electron beam from electron microscope. Different parts of scanning electron microscope (SEM) are shown in figure a below. Electron gun, electromagnetic lenses, scanning coils, detector and aperture are the main parts [91].

Working Principle

Voltage is applied to tungsten filament to generate the beam of electron from the electron gun. Negatively charges electrons are immediately move toward the anode and accelerated through the column of the SEM. The electron beam reaches the surface of the material after passing through the magnetic lenses. Resolution of SEM is determined by the condenser lenses which demagnify the beam and defines its size. The main purpose of the aperture is to stop the unwanted spray electrons [91]. The beam of electron is focused with the help of objective lens on the surface of the sample. Scan coils are used to scan

the sample across the specimen. As soon as the beam of electrons hit the surface of the material with high energy different signals are generated.

When the electron beam hit the surface of the material it can produce auger electron, X-rays and cathode luminescence. Composition of the material and the incident energy are main factors for the strength of the different signals. X-rays spectroscopy along with SEM is widely used elemental analysis technique. SEM can give better in-depth analysis and good presentable image as compared to the optical microscopy. SEM is extensively used analysis technique due to its higher resolution, greater magnification and crystallographic information [91].

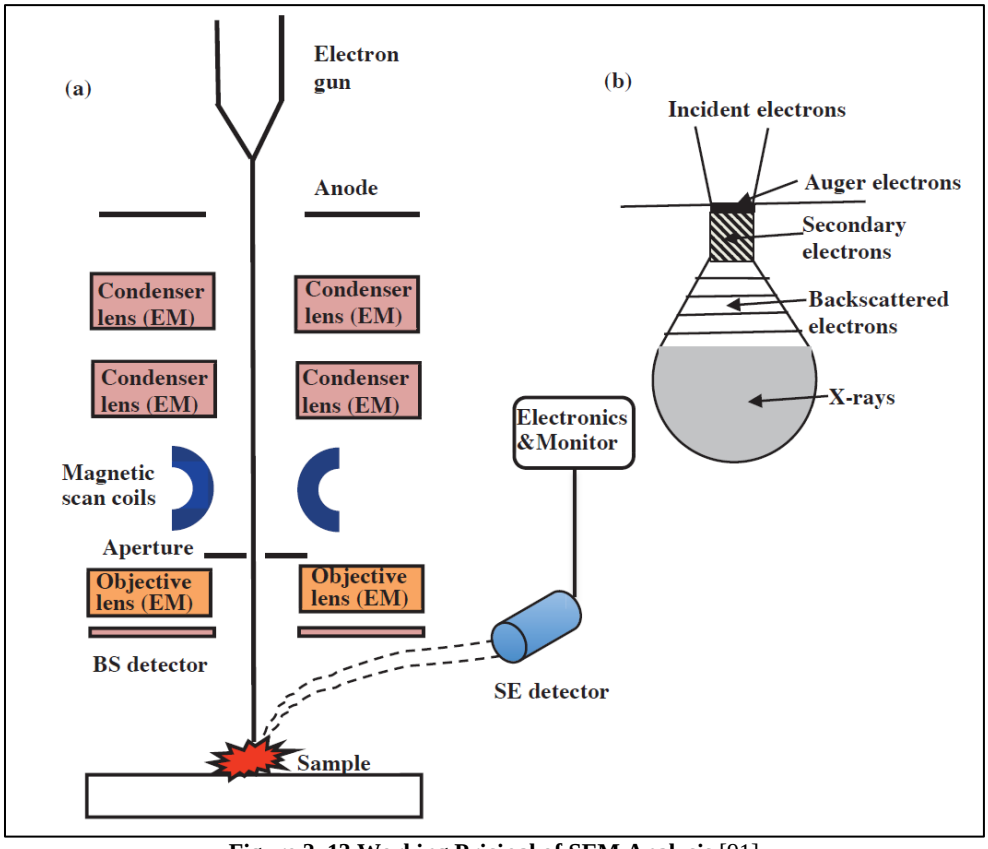

Figure 2–13 Working Pricipal of SEM Analysis [91]

2.6.4 Energy dispersive X-ray spectroscopy (EDX)

Technique most commonly used for the elemental analysis for the materials is Energy dispersive X-ray spectroscopy (EDX, EDS or EDXS). It uses electron spectroscopy for the analysis of the material. Investigation of the material is done by analyzing the X-rays emitted by the matter.

When an electron moves from the lower energy level to the higher energy level, the gap at the at the lower energy level is filled which results in emission of the characteristic X-rays containing energy between these two levels. As all the elements of the periodic table has specific X-rays and it is the characteristic of the structure of the element it helps to distinguish from each other [92].

Principle

EDX analysis is done under the electron beam bombardment. The electrons in the beam hit the electron of the material and moving them out of the shell leaving a hole behind, which is eventually filled by the electron from the higher energy level. While moving from higher level to lower level the electron releases some energy as X-ray. The amount of the energy depends on the level of transferring shell. Every element releases a unique amount of energy which is detected and used to identify the element. Generally X-ray emission increases with the increase in the atomic mass. Thus EDX is more usefully for the heavy metals [93,94].

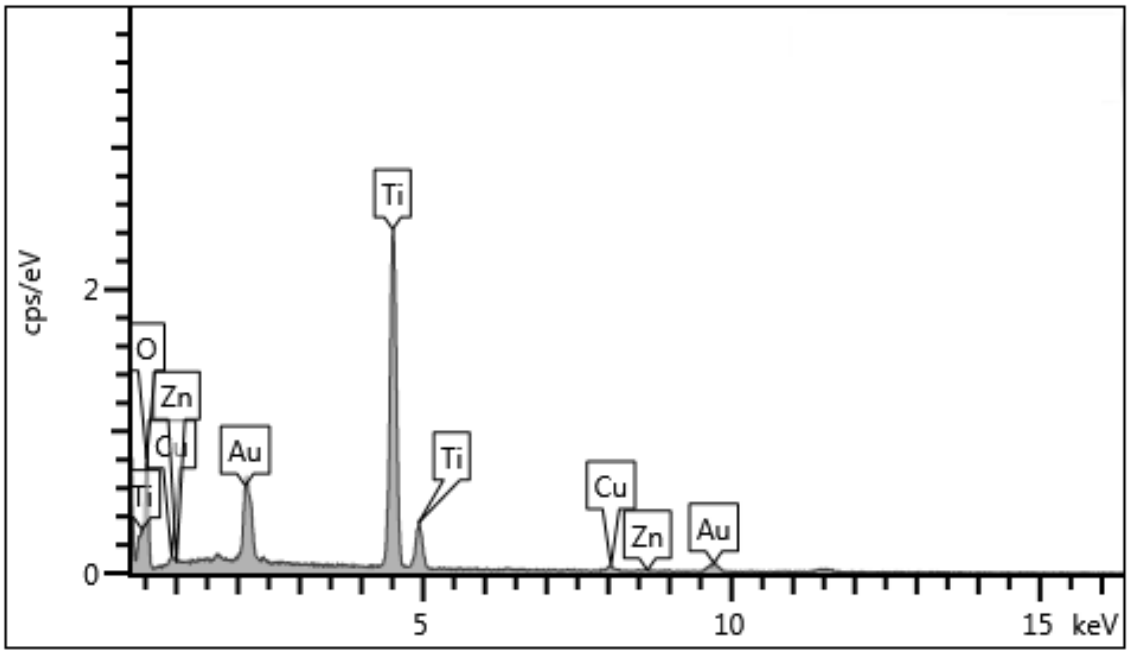

Figure 2–14 EDX Analysis Graphical Repesentation

2.6.5 Fourier Transform Infrared (FT-IR) spectroscopy

Albert Michelson designed this instrument and used it his study of relativity and light in 1887 [95]. Conventional spectroscopy is frequency domain spectroscopy but the Fourier transform spectroscopy is time domain spectroscopy. In FT-IR the radiant power data is plotted against time. The amplitude of each resolved oscillations is a function of intensity of radiation. Fourier transform is used to convert the time domain to conventional frequency domain [95].

Rotational and vibrational statuses of the molecules changes due to the absorption on the IR range. Absorption intensity and frequency is the function of photon energy transferred and vibrational energy of the molecule respectively. As a result, molecules absorb IR light and it cause change in their dipole moment. Most compounds show their characteristic IR absorption.

Conventional dispersive analysis or Fourier Transform Infrared (FT-IR) spectroscopy can be used for the analysis in the mid IR region (400-4000 cm^{-1}). FT-IR analysis is faster and better as compared to dispersive IR analysis as it give better signal to noise ratio [96] [92].

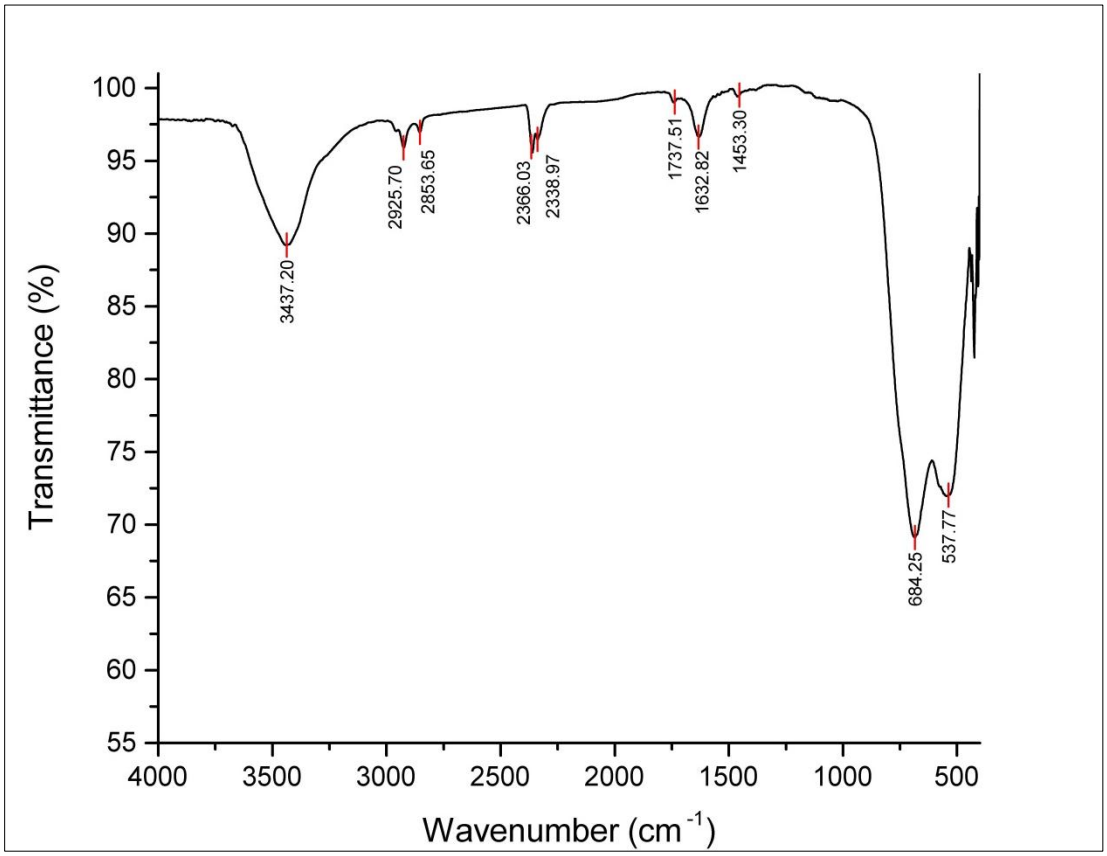

Figure 2–15 FTIR Analysis of Catalyst

2.6.6 Thermal Gravimetric Analysis (TGA)

Techniques used for the measuring the physical properties for the substance as a function of temperature in controlled temperature conditions is called thermal analysis [97].

Thermal Gravimetric Analysis (TGA) is a technique used to measure the weight loss or gain against a range of temperature. During the process of heating the material can lose

weight due to evaporation, drying or the chemical reactions that can evolve gases. Some material also showed weight increase during the process [97].

A Small amount of material is put in the alumina pan that is suspended from an analytical balance. After putting the sample the balance is zeroed and the alumina pan is heated at a certain heating rate. It instruments generates the data of the weight of the material against the time elapsed and temperature of the material. The TGA thermo grams plots the weight percent % and derivative weight % against the temperature of the reference material at X-axis [92].

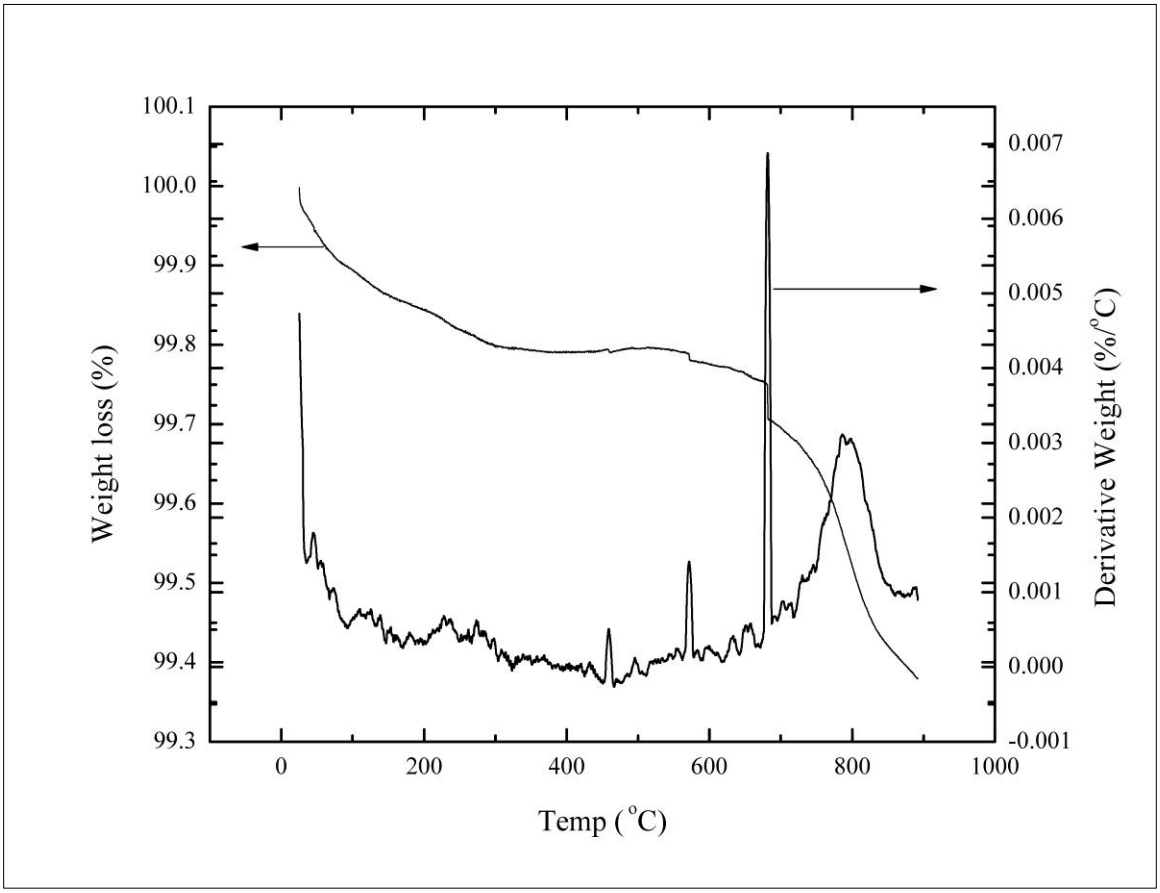

Figure 2–16 TGA Curve for the Catalyst

CHAPTER 3

MATERIAL AND METHODOLOGY

3.1 Materials

Following materials and equipment are used in the course of the reaction

1) Anatase (TiO_2)
2) Cupric Nitrate (Cu $(NO_3)_2$ $3H_2O$)
3) Zinc Nitrate (Zn $(NO_3)_2$ $10H_2O$)
4) Gas Cylinders
5) UV lamps
6) GC/MS/FID

Anatase TiO_2 was purchased from Acro Organics. Cupric Nitrate was purchased from Griffin Certified Reagent and Zinc Nitrate was purchased from Fisher Scientific Company. CO_2/H_2 mixed gas cylinder was purchased from Saudi Industrial Gas in ¼ and ½ ratios and composition was confirmed using GC/MS/FID. UV lamps of 20W were purchased. Distilled water was used to prepare all catalysts. The chemicals were used as received.

3.2 Catalyst Preparation

3.2.1 Impregnation Method

Impregnation of the porous support with solutions of the active metal components is one of the best methods for the synthesis of the heterogeneous catalyst. In impregnation method the pores of the support are filled by diffusion from the solution of the metal salt. The catalyst is synthesized either by adding the support to the solution of the active metal salt or by spraying of the support with metal salt solution; this is then followed by drying and decomposition at higher temperature, either by reduction or thermal decomposition. The support mixed in the solution containing the active metals under specifically defined condition of (time, temperature, mixing). Depending on the above mentioned conditions adsorption of the active metals occurs on the surface of the support and it results in non-uniform distribution of active metals on the support.

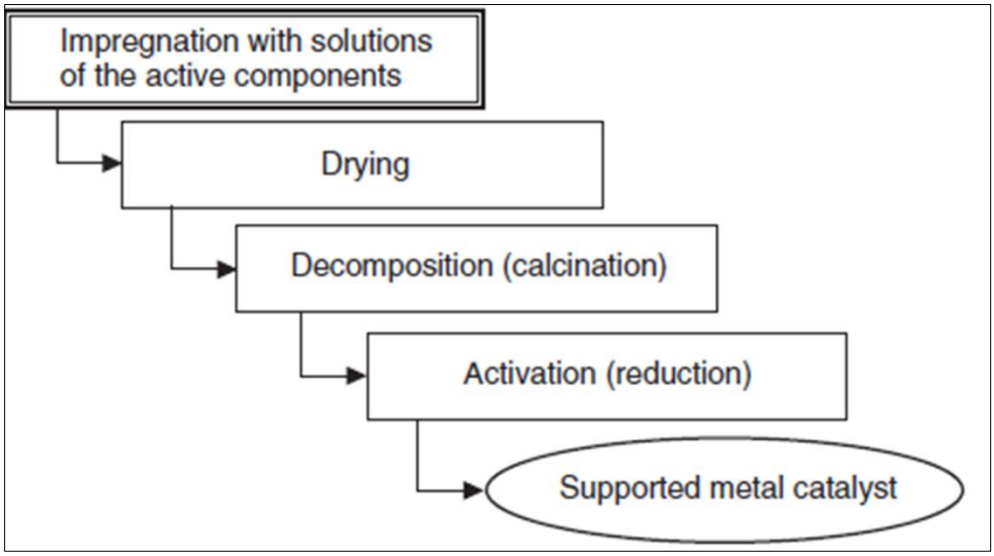

Figure 3–1 Block Diagram for the Synthesize of the catalyst

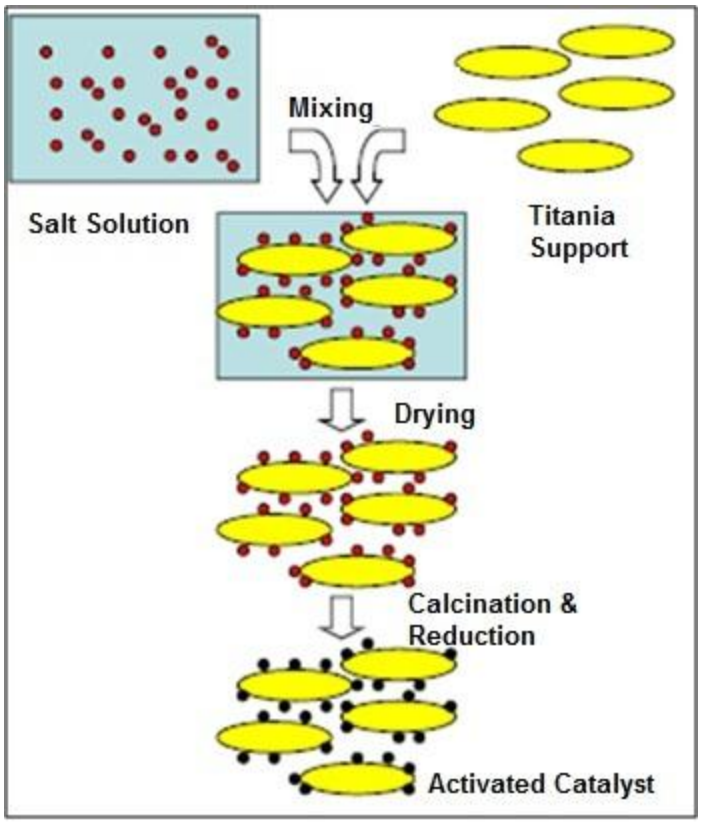

Figure 3–2 Graphical Representation of the Synthesis Process

Zn, Cu Salts and TiO_2 are precisely weighed according to the requirement and then it is mixed in distilled water. The solution is left for 24 hrs to adsorb the active metals on the surface of the support up to equilibrium concentration. After 24 hrs of adsorption the supported catalyst was filtered and dried at 110 ºC for 4 hrs. Dried powder catalyst was grinded and then placed in furnace for calcination at 380 ºC for 3 hrs. Afterwards, the catalyst was reduced by hydrogen gas at 380 ºC for 3 hrs. Final product obtained after reduction was tested for CO_2 reduction.

3.3 Catalyst Characterization

3.3.1 Bet Surface Area & Pore Volume

BET surface Area, pore volume and pore size distribution were determined using Micrometrics ASAP 2020 instrument [98]. A sample of 0.43 g treated catalyst was degassed at 573 K for 2 h under vacuum, and then N_2 gas was adsorbed–desorbed at 77 K. T-plot method was used for the determination of the micro pore volume.

3.3.2 X-Ray Diffraction (XRD)

The degree of crystallinity of the catalyst was characterized by powder X-ray diffraction (XRD) [99]. The XRD analysis was carried out by BRUKER D8 ADVANCE using Cu Kα X-Ray source (λ=1.5418 Aº) operated at 45 kV, 40 mA at 2θ angles from 20° to 80°, with a scan speed of $2°min^{-1}$.

3.3.3 Scanning Electron Microscope (SEM) & Energy-Dispersive X-Ray Spectroscopy (EDX)

JEOL Scanning Electron Microscopy (Model JSM6400) along with Energy Dispersive Spectrophotometer (EDX) operated with 20 kV voltages was used to analyze the morphology of powder catalyst samples [98]. Gold layer coating was used for the analysis. Elemental composition of the sample was determined by analyzing the X-ray spectrum generated through spot analysis.

3.3.4 Fourier Transform Infrared Spectroscopy (FTIR)

FPC FTIR Perkin Elmer spectrophotometer was used for the analysis of presence of the functional group at the surface of the catalyst. A small amount of Catalyst and 50 mg IR-grade Potassium Bromide (KBr) powder are mixed properly and hydraulically pressed at 10 ton/m^2 to prepare a thin uniform pellet [100]. The pellet was oven dried at 110 ºC to prevent any interference with moisture. All FTIR spectrums were obtained in the transmission mode. The FTIR spectrum of the pellet, % transmittance (%T) is reported against wavenumber over a range of 450 cm^{-1}–4000 cm^{-1}. It is helpful for the identification of the functional group (such as CH_3–, NO_3–, –OH, Ti–O, C–O, etc.) in the sample. The characteristic peaks indicated the presence of the functional group [101].

3.3.5 Thermo Gravimetric Analysis (TGA)

The thermo gravimetric analysis (TGA) was carried out using the TA instrument SDT Q600 to determine the thermal stability of the catalyst materials prior to calcination. The rate of heating was maintained at 10 ºC/min, and the measurement was carried out from 25 ºC to 900 ºC with N_2 flowing at a rate of 100 mL/min. TGA results are reported as thermo grams which are plots of the percentage decomposition of the catalyst versus temperature [101].

3.4 Photo Reduction Experiments

The system was irradiated by 3 lamps of 20 W each with a peak light intensity at 254 nm. The whole system was covered by aluminum foil to prevent any interference of light. The glass column is placed in between the triangle of lamps.

Glass column of diameter 0.5 cm and length of 30 cm was used during the course of the reaction. Column was filled with 1 g of catalyst. 5 mL/min gas mixture was introduced in the column and allowed to pass for 30 min under UV light at STP. Sample was collected after 30 min using a syringe for analysis from the outlet of the glass column and introduced into the GS/MS/FID. The analysis shows that CO_2 was successfully converted to hydrocarbons and percent conversion was calculated based on the amount of CO_2 consumed.

$$\%\ CO_2\ Conversion = \frac{CO_{2_{in}} - CO_{2_{out}}}{CO_{2_{in}}} * 100$$

CHAPTER 4

RESULTS AND DISCUSSION

4.1 Catalyst Characterization

4.1.1 Particle Size Distribution

Table 4-1 summarizes the properties of the catalyst. The specific surface area (S_{BET}) of Cu-Zn/TiO_2 and TiO_2 are 8.59 and 10 m^2/g respectively. It shows that the impregnation of the Cu-Zn on the surface of TiO_2 has reduced the surface area.

Table 4-1 Surface properties of catalyst

Catalyst	Surface Area (m^2/g)	Pore Volume (cm^3/g)	Pore Size (nm)
TiO_2	10	0.000888	2.013
25% Cu 10% Zn/TiO_2	8.59	0.000708	2.019

The nitrogen adsorption-desorption isotherms and pore size distribution curves of Cu-Zn/TiO_2 catalyst are shown in Figure 4–1Figure 2–10 N_2 Adsorptiom Isotherms. According to IUPAC classification, it exhibited type III isotherms [102–104], which are typical characteristics of mesoporous material [102–105] . As per classification by IUPAC, the type of hysteresis loop is H3 [103,104]. This type of hysteresis is usually found on solids consisting of agglomerates or aggregates of particles forming slit shaped

pores (plates or edged particles like cubes) [99,103,104]. The average pore size and BET surface area of 25% Cu 10% Zn/TiO_2 were found to be about 2.02 nm and 8.59 m^2/g. The value of BET surface area for Cu-Zn/TiO2 is near to bare TiO_2 nanoparticles it shows that the impregnation method does not have a considerable effect on the surface area of the catalyst [102]. Pore size distribution of the Cu-Zn/TiO_2 nanoparticles was obtained from adsorption branch, using the BJH method in the Figure 4–2 in the range of 1.5–10 nm [102]. The major pore size is 2.83 nm.

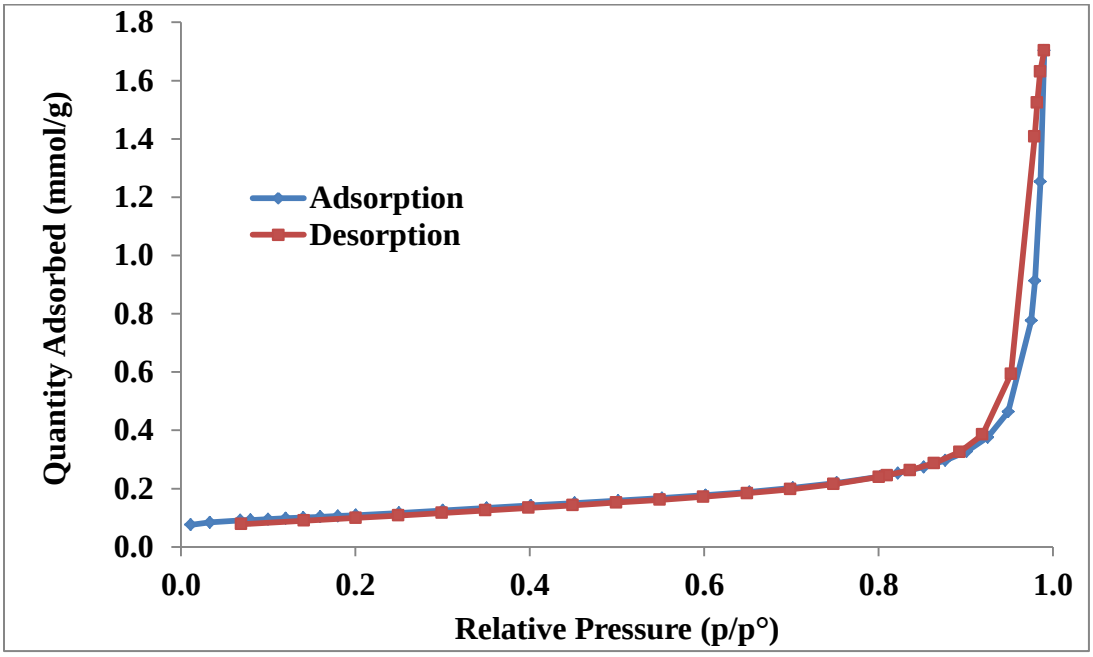

Figure 4–1 N_2 isotherm adsorption-desorption curves for Synthesized Catalyst

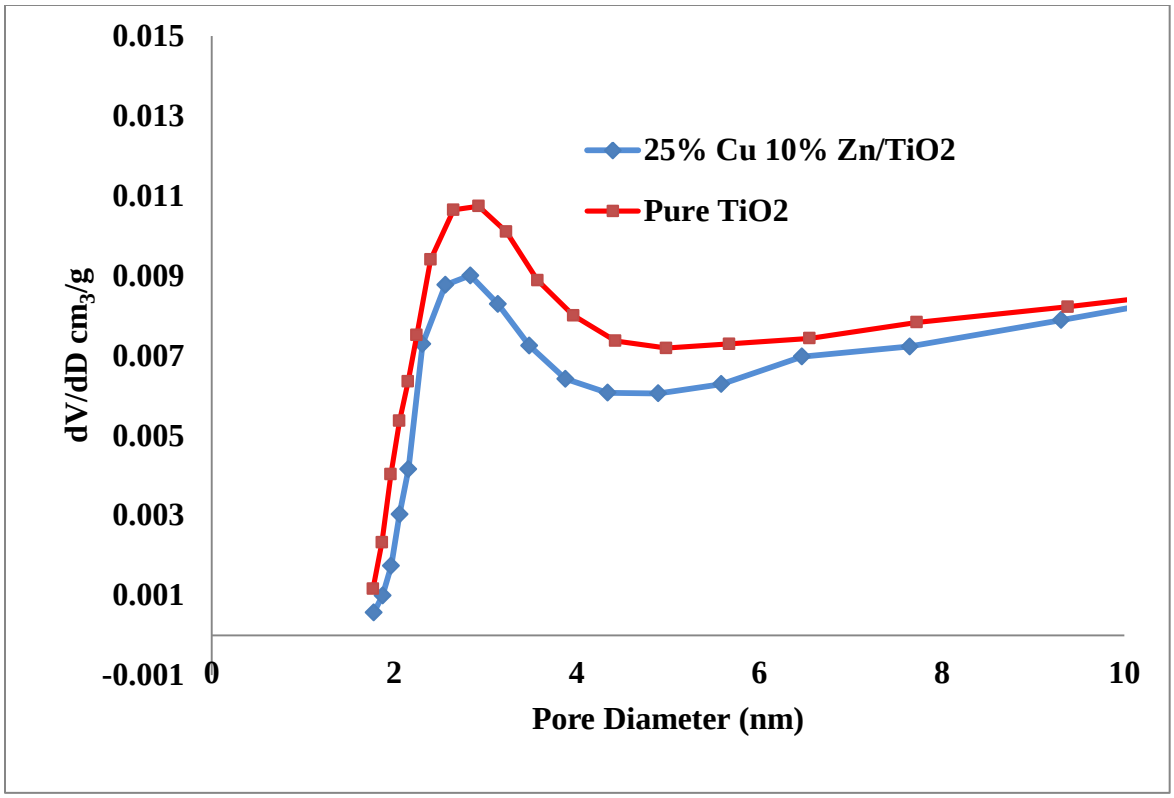

Figure 4–2 Pore Size Distribution of Synthesized Catalyst

4.1.2 Scanning Electron Microscopy (SEM)

The morphology of the synthesized catalyst was observed by SEM as shown in the figures below of different sites and different magnifications i.e. 0.5 µ, 1µ and 2 µ. Morphology and elemental composition of the catalyst was examined by scanning electron microscopy (SEM) . The results are similar to those presented by H. Ninsonti et.al [106] showing rough morphology and slight agglomeration. Similarly results are in accordance with the results presented by M. a. Behnajady et.al [102] that there is uniform distribution of the particles with spherical morphology and slight agglomeration.

The deposited clusters of Zn and Cu on the surface of TiO_2 indicate the week interaction of Cu and Zn with the support prepared by the impregnation method [101]. The slight agglomeration present on the surface might be due to the sintering during the calcination process [100].

Increasing Cu and Zn loading has increased the crystalline size and decreased the BET surface area similar to the work reported by Ganesh et.al [107]. The bare TiO_2 and impregnated TiO_2 has almost the same common features showing spherical like morphology [108]. Agglomeration of the smaller particles is due to the Ostwald ripening mechanism of the coarsening and aggregation which competes with nucleation during hydrolysis [109].

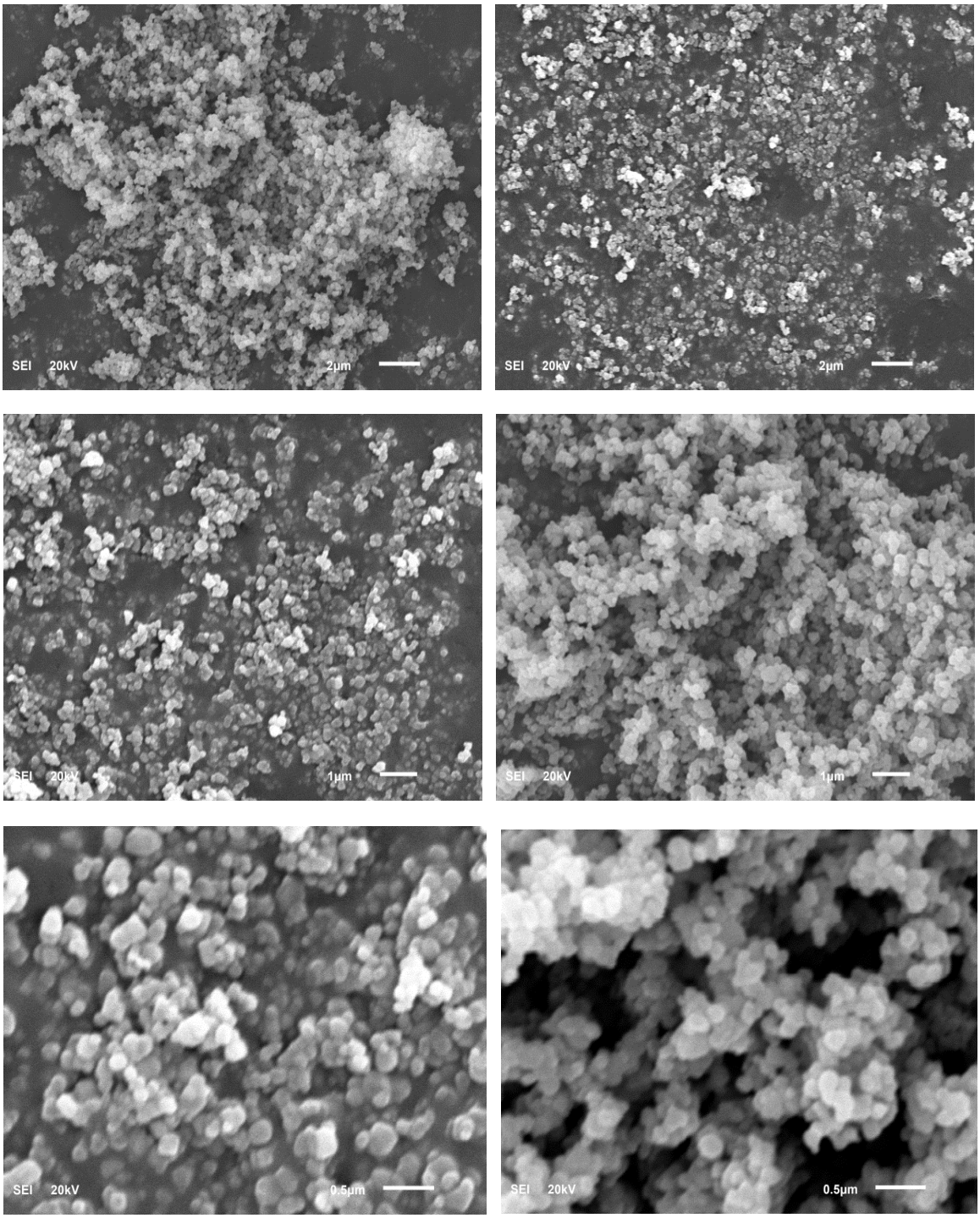

Figure 4–3 SEM images at different resolution for the Synthesized Catalyst

4.1.3 Energy Dispersive X-Ray spectrum (EDX)

The EDX result proved the existence of the Cu and Zn on the surface of the TiO_2. The peaks of copper, zinc and titanium are quite specific in Figure 4. The EDX spectrum Figure 4–4 shows the characteristic peak at 4.5 keV and 4.9 keV, confirming the presence of titanium [110]. Similarly characteristic peaks at 8.04 KeV and 0.93 KeV, confirms the presence of Copper and peaks at 8.63 KeV and 1.012 KeV indicate the presence of Zn in the survey area of the sample [111]. EDX analysis and the spectra of 2.6% Cu 0.5 % Zn/TiO2 is shown in Figure 4–4 which gave both qualitative and quantitative information [112] shown in Table 4-2

Table 4-2 Energy dispersive X-ray elemental and atomic analysis

Catalyst	O	Ti	Cu	Zn	Total
25% Cu 10% Zn/TiO2	56.30	40.60	2.6	0.5	100

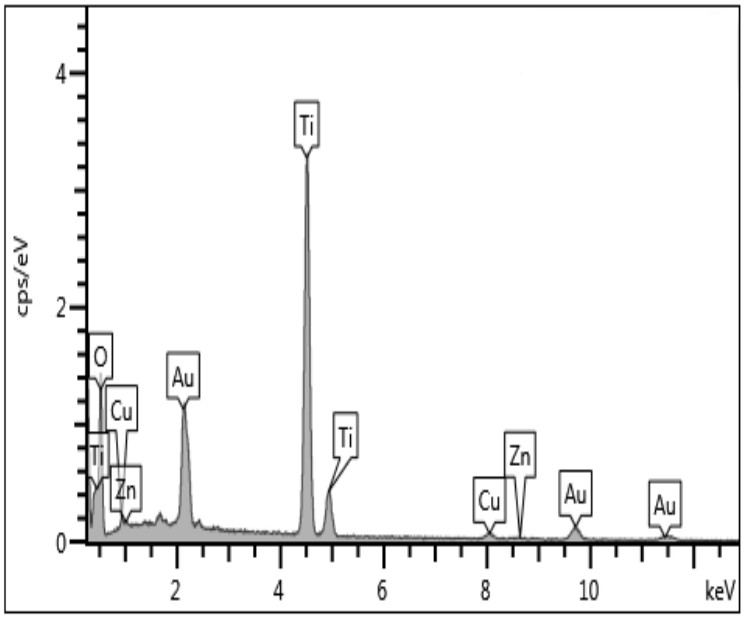

Figure 4–4 EDX analysis of the Synthesized Catalyst

4.1.4 X-Ray Diffraction (XRD)

X-ray powder diffraction (XRD) is an analytical technique mainly used for phase identification of a powder crystalline material. XRD analysis of 25% Cu 10% Zn/TiO_2 is presented in the Figure 4–5. The major peak at 2θ ~ 25.33, 37.8, 48.06, 53.9 and 55.08 represents the TiO_2 (Anatase phase) (JCPDS 84-1286) [113,114]. Metallic copper is detected on the metal surface and shown as the characteristic peak at 2θ ~ 43.6 and 75.06 which are in accordance with the metallic copper (JCPDS NO.04-0836) [115–117]. Amorphous phase of CuO had also been detected at its characteristic peaks 2θ ~ 62.70 and 68.78 almost similar to the CuO (JCPDS file No. 05-661) [118–120]. Similarly small peaks of metallic Zn are shown in Figure 4–5 The positions of the peaks are in accordance with the JCPDS card number 04-0831 at 2θ~ 36.9 and 38.6 [121–124]. The diffraction peaks found at 2θ~70.06 is indexed at hexagonal wurtzite phase and it is almost similar to ZnO JPCDS 36-1451 [125–128].

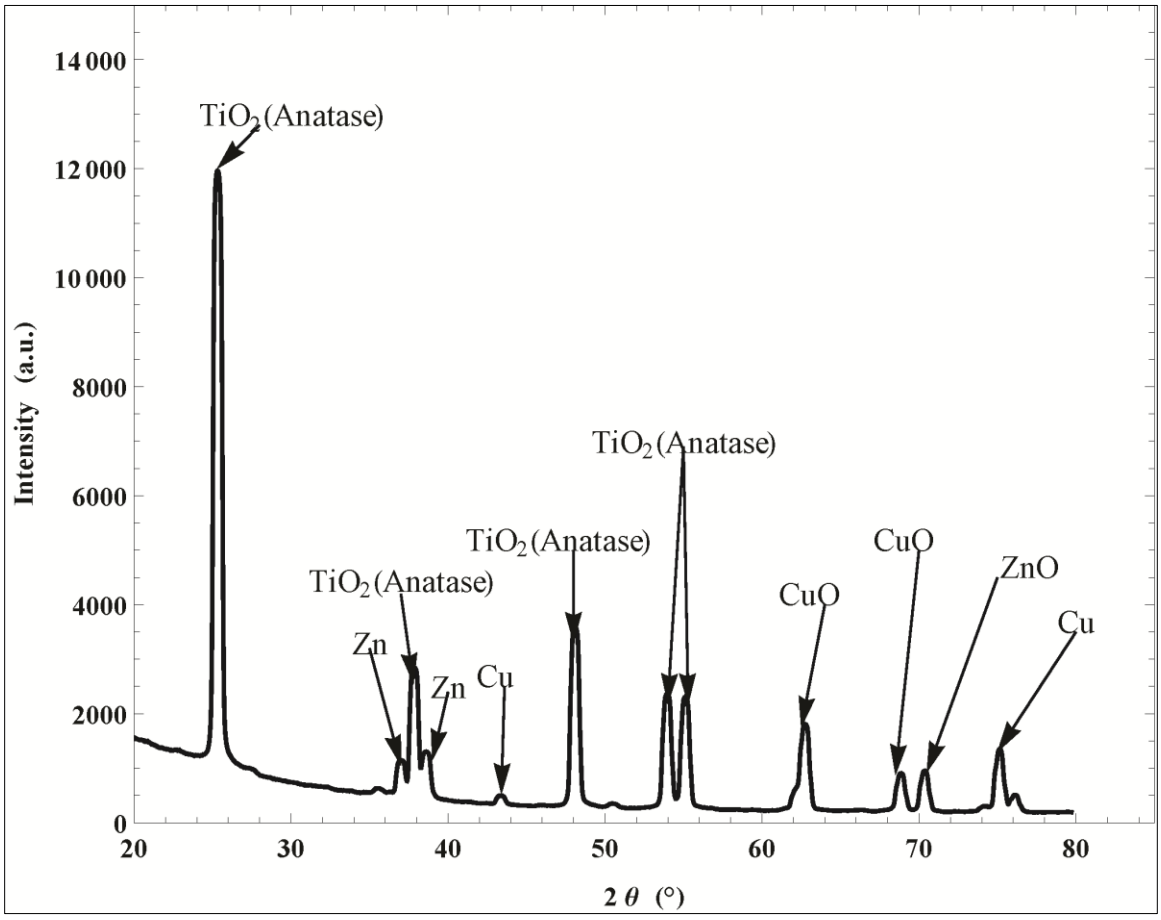

Figure 4–5 XRD Analysis of the Synthesized Catalyst

4.1.5 Fourier Transform Infrared Spectroscopy (FTIR)

The FT-IR absorption spectrum of 25% Cu 10% Zn/TiO_2 is shown in Figure 4–6. In the spectra below, absorption peak at 1636 cm^{-1} to 3437-3440 cm^{-1} are attributed to O-H bending, hydroxyl group and water physically adsorbed , respectively [101,104,129]. The IR band observed from 400 to 900 cm^{-1} corresponds to Ti-O stretching vibrations [100,101,130]. The broad IR peaks at 2350 cm^{-1} represent the CO_2 asymmetric stretch [131–134]. IR peaks at 2924 cm^{-1} and 2850 cm^{-1} represent the C-H stretching [135,136] 2924 cm^{-1} represent the asymmetric and 2850 cm^{-1} represent the symmetric vibrations [135,137].

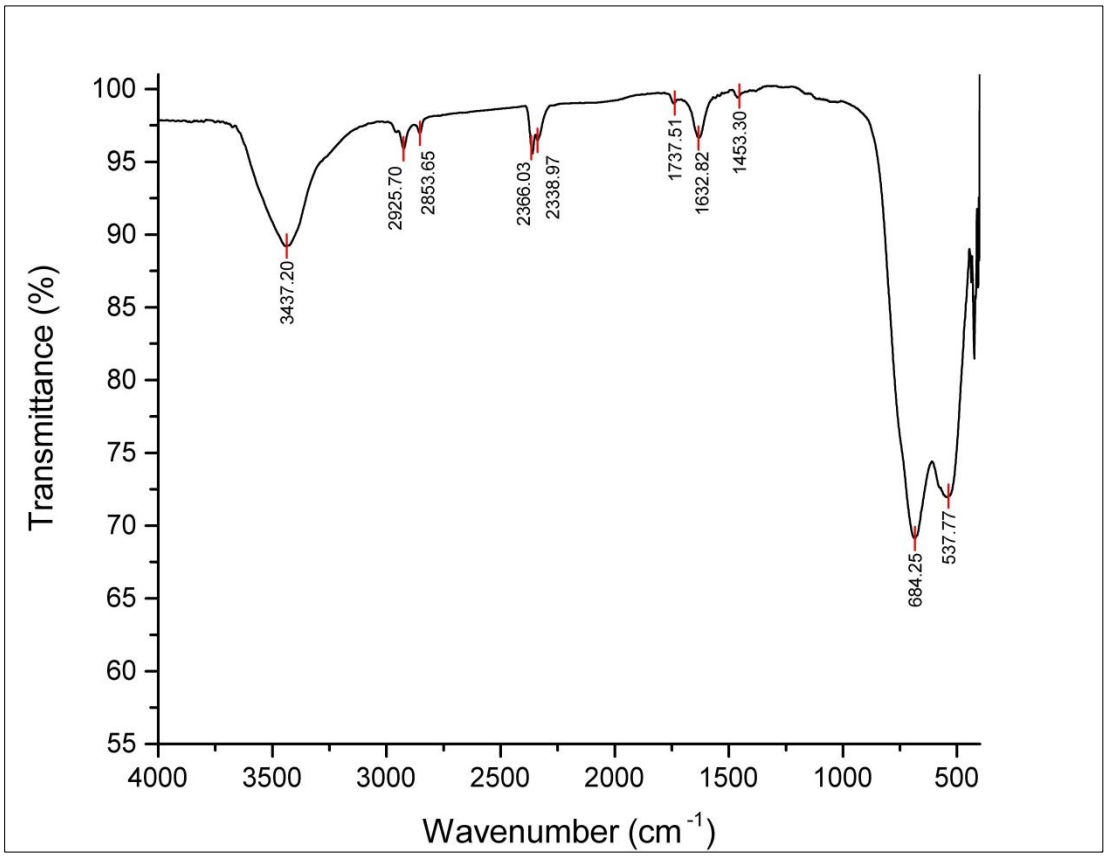

Figure 4–6 FTIR Analysis of Synthesized Catalyst

4.1.6 Thermal Gravimetric Analysis (TGA)

The TGA curve of the 25% Cu 10% Zn / TiO_2 is shown in the Figure 4–7. The material is thermally stable and the total weight loss is less than 1%. Gradual weight loss till the 200 is due to the little moisture present in material. Weight loss above 600 °C indicates desorption of surface species

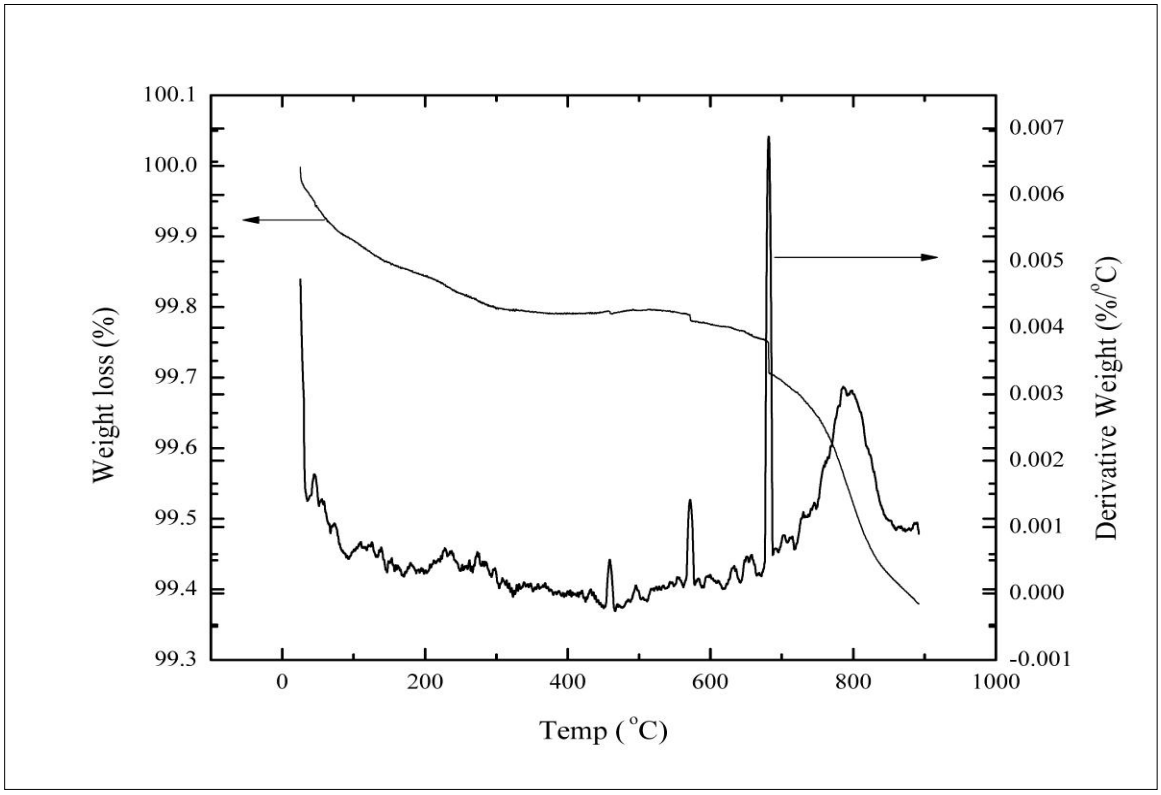

Figure 4–7 TGA Analysis of Synthesized Catalyst

4.2 Photocatalytic conversion Experiments

As described in previous chapter, metal modified TiO_2 was synthesized via wet impregnation process in this research. These synthesized catalysts were characterized by using different analytical techniques and data of these techniques is presented in previous section. In this section, the results of the experiments and the effects of various parameters are presented.

4.2.1 Effect of Cu Modified TiO_2

The effect of Cu loading on the conversion of CO_2 for Cu/TiO_2 was studied by loading different weight concentrations of Cu 0%, 15%, 25%, 35%. At each Cu loading the experiments were performed and repeated to confirm the reproducibility of the results. The results are shown in the Figure 4–8. It clearly shows that 25% Cu loading by weight has the highest conversion. Decreasing or increasing the impregnated weight % of Cu to 15% or increasing it to 35 % reduced the conversions. Similar results are reported in literature that there is an optimum Cu loading for CO_2 photo reduction on TiO_2 based catalysts [3,71,138–140]. At lower Cu loading content below the optimum value, TiO_2 did not contain sufficient electron trap sites that can inhibit the recombination of electrons and hole pairs, thus leading to lower photo activity [3][139][141].

However, at higher Cu loading than optimum value could decrease the catalytic activity due to the increased Cu amount can block the light absorption centers of TiO_2 [3] and excess Cu species could create the options for the recombination of the photo induced electron and the holes, as a result decrease the photo activity [138,139,141].

Table 4-3 Effect of Cu %age on Conversion for CO_2

Catalyst	Conversion at 4/1	Conversion at 2/1
TiO_2	9.65	7.5
15% Cu/TiO_2	13.2	11.03
25% Cu/TiO_2	13.35	12.52
35% Cu/TiO_2	10	8

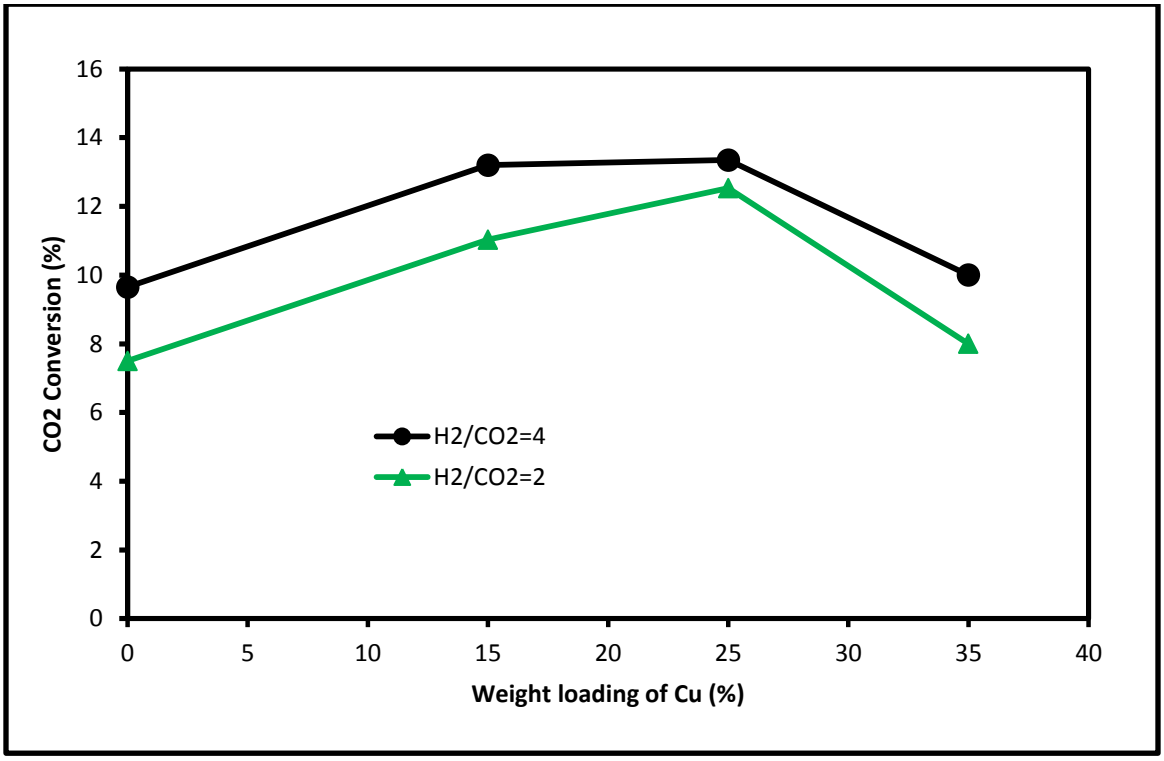

Figure 4–8 Effect of % age of Cu on the Conversion of CO_2 for Synthesized Catalyst

4.2.2 Effect of Zn Loading in Cu-Zn/TiO_2 catalyst

Photo reduction of CO_2 with H_2 using Cu-Zn/TiO_2 based was studied. Conversion of CO_2 as a function of metal loading is plotted in Figure 4–9. Different catalysts under UV light irradiations were tested and the experiments were repeated to confirm the reproducibility of the results. The experiments were conducted at two different ratios H_2/CO_2 4 and 1. All the experiments were conducted for 30 min irradiation time and flow rate of 5 mL/min at 1 bar pressure and room temperature. All the catalyst impregnated with Cu and Zn showed the conversion of CO_2 under the UV light irradiations. Two series of catalyst were tested to study the effect of the metal catalyst loading on the catalyst efficiency. In first type of series, the weight of the Cu metal loading is kept constant at 15% and the weight of the Zn metal loading is changed from 5% to 25%. In second type of the series, Zn metal loading is kept constant at 15% and the Cu metal loading is changed from 5% to 25%. In Figure 4–9, the results of the first type of series with constant copper loading are shown. The catalyst with 5% Zn loading appeared to be the best among the others co-modified TiO_2, while the others co-modified catalysts showed less conversion as compared to 15% Cu-5% Zn/TiO_2 catalyst. The Cu species deposited on the surface of the catalyst work as hole scavengers and as a result enhance the CO_2 reduction. The dispersion of the Cu has a positive effect on the conversion rate. The possible reason behind the decreasing trend of the conversion is by increasing the amount of Zn on the surface of catalyst we are increasing the band gap of the overall system because Zn has higher band gap than Cu. Secondly Zn has lower thermal conductivity than that of Cu so by increasing the amount of Zn the overall conductivity of the system started to decrease and results in the decrease in the conversion of CO_2.

Table 4-4 Effect of Zn Loading on Cu-Zn/TiO_2 catalyst

Catalyst	Conversion at 4/1	Conversion at 2/1
15% Cu 5% Zn/TiO_2	12.05	10.41
15% Cu 10% Zn/TiO_2	10.2	9.64
15% Cu 15% Zn/TiO_2	9.5	9.22
15% Cu 20% Zn/TiO_2	8.25	7.94
15% Cu 25% Zn/TiO_2	6.2	5.88

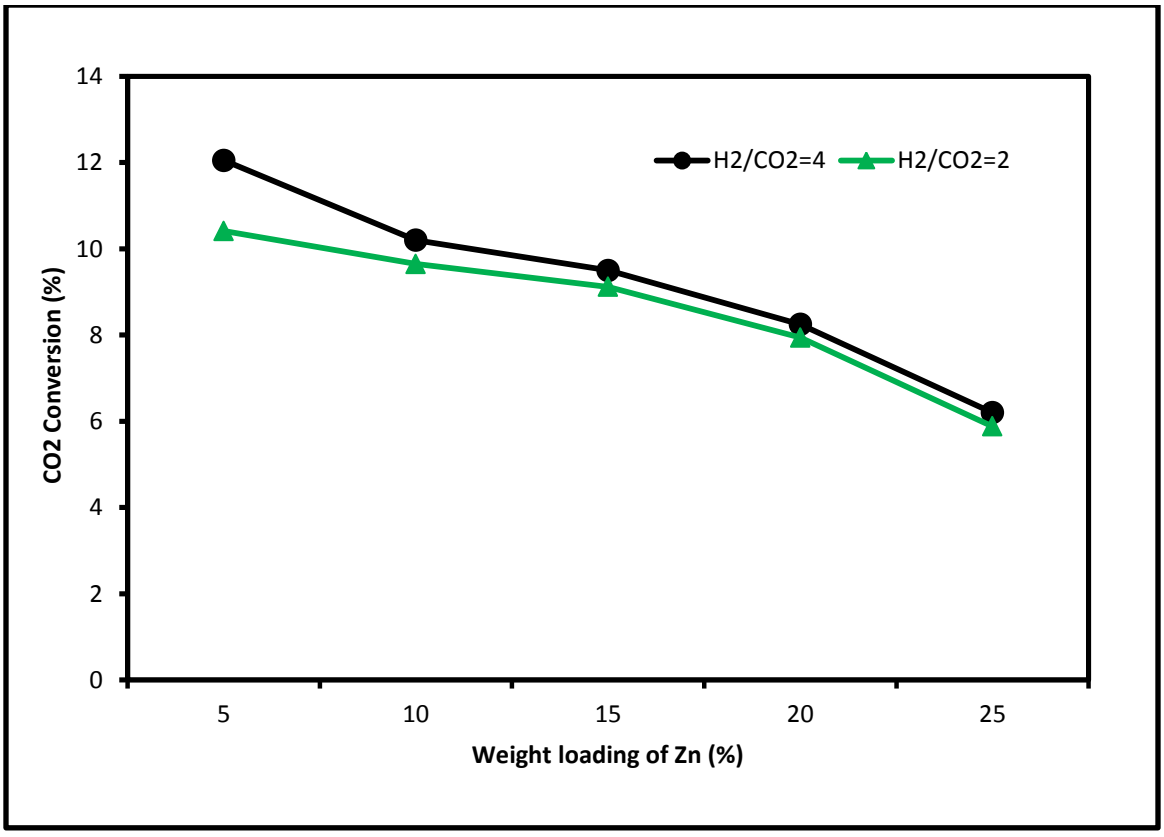

Figure 4–9 Effect of % age of Zn on the Conversion with Constant Cu (15%)

4.2.3 Effect of Cu Loading in Cu-Zn/TiO_2 catalyst

In the Figure 4–10 the results of the second type of series with constant Zn loading is shown. The Zn loading is kept constant at a value of 15% with changing Cu from the value of 5% to the 25 %. The catalyst with the 5% Cu and 15 % Zn on the surface of the catalyst surface appeared to be the best among all the other Co modified catalysts in this series. The 5% Cu and 15 % Zn catalyst showed maximum conversion of 12.2 % at 4/1 ratio of H_2 to CO_2. The catalyst without any Cu and having only the Zn on the surface of the TiO_2 showed less conversion around 10% which increased with the addition of Cu to the catalyst but after a certain value the conversion of the catalyst started to decrease.

Possible reason for the first increase of the conversion with addition of Cu to the catalyst is that Cu act as hole scavenger and electron trapper in the catalyst and as a result will enhance the conversion efficiency of the catalyst. Secondly at low amount of Cu the dispersion of Cu is better and it eventually enhances the reduction rate of the CO_2.

On the other hand, the decrease in the conversion efficiency after the optimum catalyst for this series has many reasons as well. At low Cu content, it hinders the recombination of the electron and holes but as the Cu content increase above the optimum level the Cu species became the recombination centers for the photo induced electrons and the hole resulting in the decrease of the photocatalytic activity of the catalyst. Other suggested reason can be the size difference of Cu and Zn and as reported in literature the introduction of Cu can affect the Zn.

Table 4-5 Effect of Cu Loading on Cu-Zn/TiO_2 catalyst

Catalyst	Conversion at 4/1	Conversion at 2/1
15% Zn/TiO_2	10.3	10
5% Cu 15% Zn/ TiO_2	12.2	12
10% Cu 15% Zn/ TiO_2	11.5	10.3
15% Cu 15% Zn/ TiO_2	9.5	9.11
20% Cu 15% Zn/ TiO_2	6.3	5.32
25% Cu 15% Zn/ TiO_2	6.25	4.41

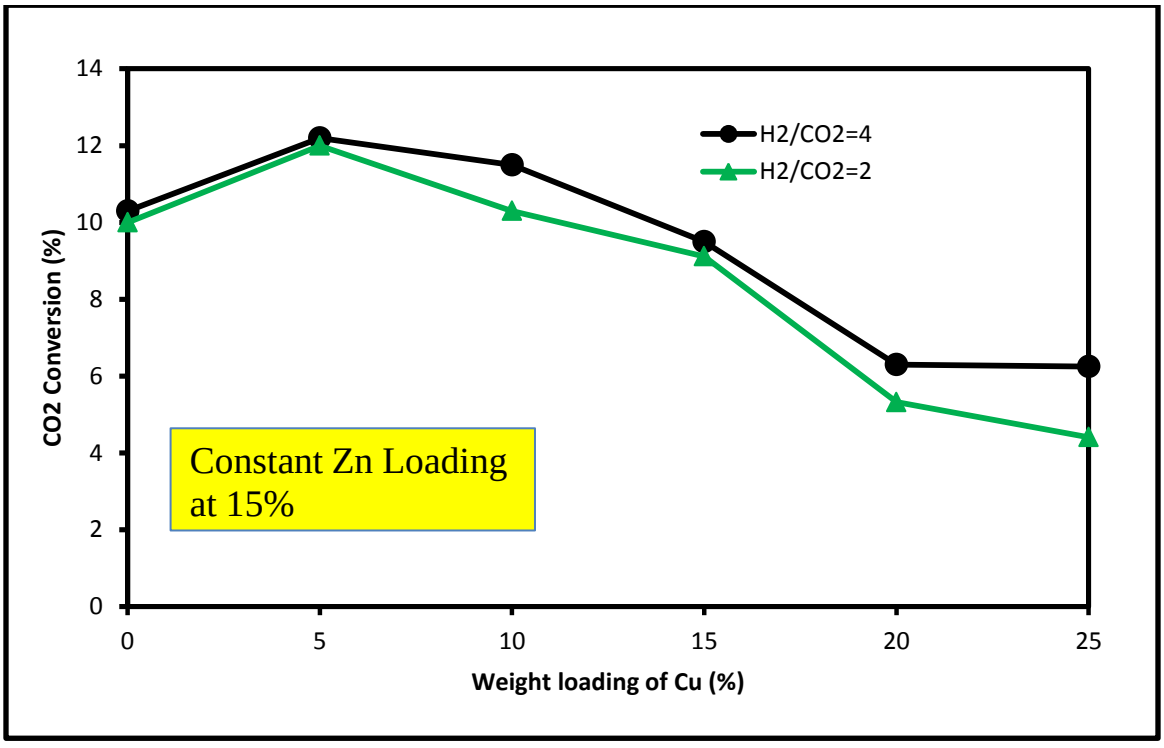

Figure 4–10 Effect of % age of Cu on the Conversion with Constant Zn (15%)

4.2.4 Optimum Cu-Zn/TiO_2 Catalyst for Photocatalytic Conversion of CO_2

The best catalyst is found to be the one having less Zn and more Cu content. It is evident from the results that increasing the Zn decrease the conversion and increasing the Cu content increase the conversion up to certain optimum value after that conversion started to decrease.

The catalyst 25% Cu and 10% Zn over the surface of TiO_2 proved to the best catalyst for the photocatalytic conversion of CO_2 in the whole system of the catalysts we tested for this research. This catalyst showed 14.3% conversion of CO_2 at the operating condition mentioned in the experimental section. Conversion at H_2/CO_2 ratio 2/1 is slightly lower than at 4/1. All the characterization presented and discussed above are of this catalyst. This value of Zinc seems to be optimum so we test with different loadings of Cu ranging from 15% to 35% at same condition. At the Cu loading less than the optimum the conversion is less and after the optimum the conversion also decreases at both ratios. Results are presented in Table 4-6 and shown in Figure 4–11

The reasons behind the decrease were discussed earlier as well e.g. at higher Cu concentration it becomes the recombination centers for the holes and the photo induced electron and more concentration also cause the blockage of the light absorption centers of TiO_2 resulting in the decreased activity of the catalyst. Higher conversion at the low Cu content is due to the better dispersion of the Cu on the surface of the catalyst. Compared to low Cu loading it inhibits the recombination of the electrons and the hole work as the electron trapper for the photo induced electron.

Table 4-6 Effect of Cu-Zn/TiO_2 catalyst on Conversion

Catalyst	Conversion at 4/1	Conversion at 2/1
15% Cu 10% Zn/TiO_2	10.2	9.64
20% Cu 10% Zn/TiO_2	10.4	7.35
25% Cu 10% Zn/TiO_2	14.3	14
30% Cu 10% Zn/TiO_2	10	9.64
35% Cu 10% Zn/TiO_2	8.5	6.58

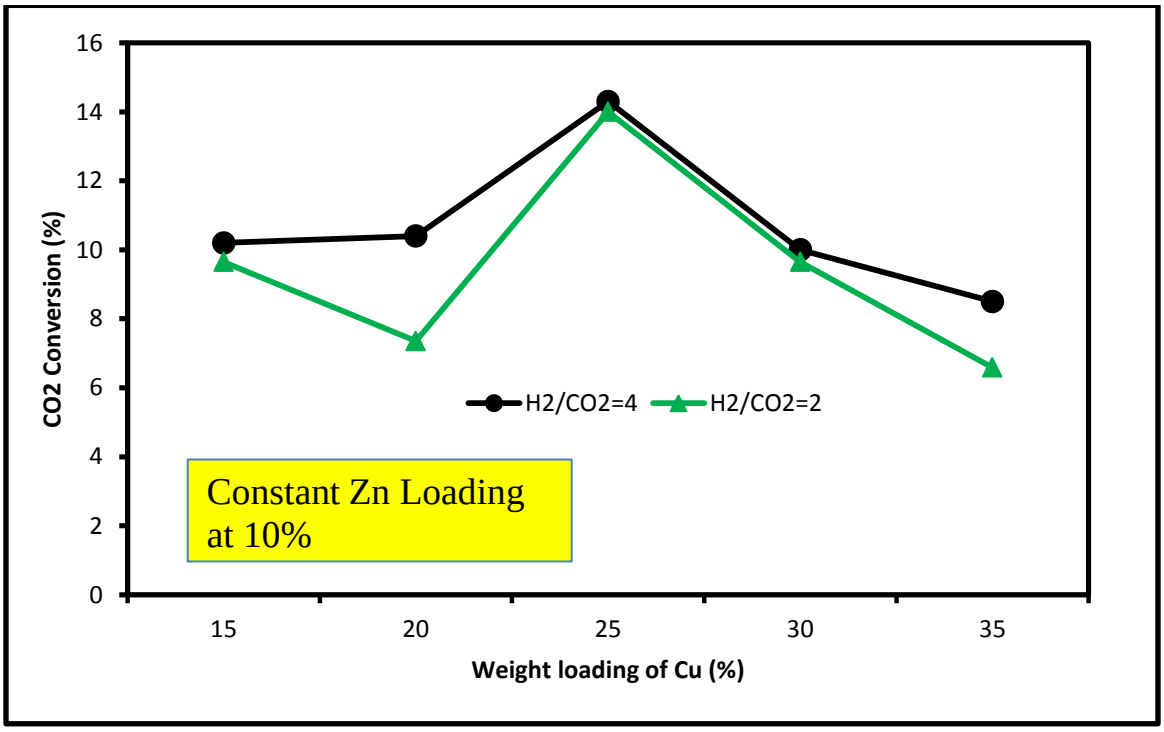

Figure 4–11 Effect of Cu-Zn/TiO2 catalyst on CO_2 Conversion

4.2.5 Synergistic effect of Cu-Zn/TiO_2

It is reported above that Cu and Zn over TiO_2 has managed to improve the catalytic conversion of CO_2. When the TiO_2 is simultaneously modified with Cu and Zn at a certain it is seen that it increase the results synergistically. It is shown in the figure below that the bare TiO_2 showed 9.65 % conversion at 4/1 which increased 48% when co modified TiO_2 is used. Similarly the co modified catalyst has the higher conversion than that of separately modified TiO_2 with Zn and Cu. The co modified TiO_2 has 38% and 8% more conversion that that of Zn and Cu modified TiO_2, respectively. It is observed from the results that to achieve an optimum activity, a higher modifier concentration is needed under UV light irradiation in case of Cu. There is no noticeable enhancement in the conversion of Zn impregnated TiO_2 as the conduction band of the Zn is almost the same as that of TiO_2 so Zn unable to act as electron trap. Hence the presence of Zn with 15% wt, was not able to enhance the activity of TiO_2 for CO_2 photo reduction, even though Cu with the same wt% has shown the significant increase in the conversion.

Table 4-7 Synergetic Effect of Cu-Zn/TiO_2

Catalyst	Conversion at 4/1	Conversion at 2/1
TiO_2	9.65	7.5
Zn/TiO_2	10.3	10
Cu/TiO_2	13.2	11.02
$Cu\text{-}Zn/TiO_2$	14.3	14

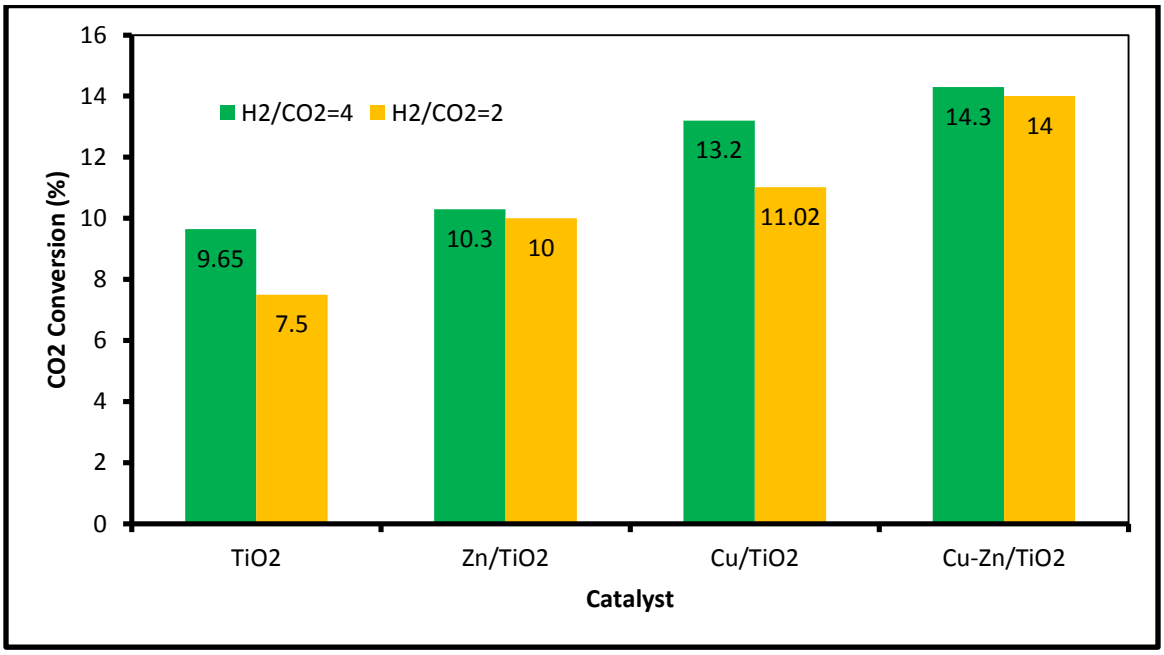

Figure 4–12 Synergetic Effect of Cu-Zn/TiO_2

4.2.6 Effect of Time on the Conversion of the Catalyst

All catalyst deactivate with time. As a general behavior in long term reaction the activity of the catalyst decreases as a function of time. The conversion of the catalyst increase with time until it reaches the highest value of 12.2 % after 90 min. After that the conversion started to decrease and reaches the zero after 180 min. One of the suggested reasons behind decrease in the photocatalytic activity is effect of the temperature on the adsorption of the species on the surface of the catalyst. The hypothesis is based on the fact that adsorption on the catalyst surface is the main factor for the reaction of the species at the surface of the catalyst and eventually the conversion to the products. As the temperature of the lamps takes 60 min to reach a plateau of highest temperature so the gas adsorption is inhibited as a function of time and as a result the activity of the catalyst decreases [142]. Other reasons for the lowering of the photocatalytic activity of the catalyst can be coagulation and the saturation of the adsorption site with the intermediate products [60]. Reduction of the active sites with time and usage of the catalyst is also one of the major reasons for the reduction of the activity of the catalyst. Deterioration of the catalyst site with the moisture and other products cannot be neglected as well.

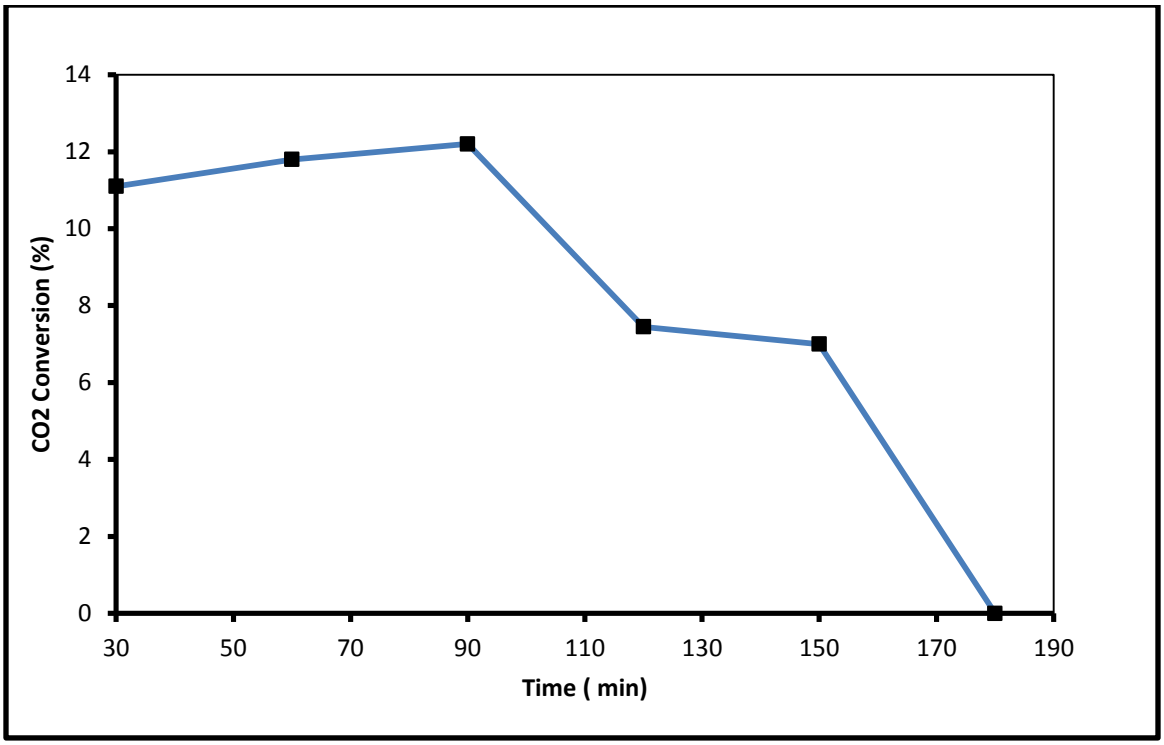

Figure 4–13 Time Dependence Cu-Zn/TiO_2 Catalyst of CO_2Conversion

CHAPTER 5

CONCLUSIONS AND RECOMMENDATIONS

5.1 Conclusions

1) A series of catalysts were synthesized as per requirement
2) The aim was to impregnate the support with metal catalyst and this aim was achieved using wet impregnation technique and the presence of the impregnated metals is confirmed using XRD and EDX analysis techniques
3) The synthesized catalyst is thermally stable as the thermal stability of the catalyst is tested using TGA analysis
4) The conversion of the CO_2 was increased to 13.35 % as we increase the amount of Cu on the surface of the support.
5) Increasing the Zn on the surface of the catalyst has nominal effect on the conversion of CO_2
6) Synergetic effect for the conversion for CO_2 was observed when 25% Cu and 10% Zn was impregnated on the surface of the support and the resulted conversion is 14.3%.
7) H_2/CO_2=4/1 showed better conversion than H_2/CO_2=2/1
8) The catalyst deactivates after 3 hr and need to be regenerated for further use.

5.2 Recommendations

1) We have used the wet impregnation method for the preparation of the catalyst so it is recommended to using other techniques like Sol gel and incipient wetness for the preparation of catalyst
2) We have tested the catalyst in the presence of UV light for the conversion of CO_2 it is recommended to use other light sources especially solar light.
3) We have impregnated the Cu and Zn on the surface of the support it is recommended to use other pair of metal oxide to increase the conversion. i.e. Nickel (Ni), Cerium (Ce) etc.
4) We have used a fixed amount of light and it is highly recommended to use the higher intensity of light to increase the conversion
5) The reactor should be designed in such a way that we can harvest maximum amount of light emitting from the light lamps.

References

[1] X. Chang, J. Zheng, M. a. Gondal, G. Ji, Res. Chem. Intermed. (2013).

[2] P.-Y. Liou, S.-C. Chen, J.C.S. Wu, D. Liu, S. Mackintosh, M. Maroto-Valer, R. Linforth, Energy Environ. Sci. 4 (2011) 1487.

[3] I. Tseng, W. Chang, J. Wu, Appl. Catal. B Environ. 37 (2002) 37.

[4] M. Tajmehr, F. Rahimpour, S. Sharifnia, (2012) 29.

[5] S.C. Roy, O.K. Varghese, M. Paulose, C.A. Grimes, 4 (2010) 1259.

[6] E.A. Laws, J.L. Berning, Bioresour. Technol. 37 (1991) 25.

[7] L. Bernstein, P. Bosch, O. Canziani, Z. Chen, R. Christ, O. Davidson, W. Hare, S. Huq, D. Karoly, V. Kattsov, Z. Kundzewicz, J. Liu, U. Lohmann, M. Manning, T. Matsuno, B. Menne, B. Metz, M. Mirza, N. Nicholls, L. Nurse, R. Pachauri, J. Palutikof, M. Parry, D. Qin, N. Ravindranath, A. Reisinger, J. Ren, K. Riahi, C. Rosenzweig, M. Rusticucci, S. Sch-Neider, Y. Sokona, S. Solomon, P. Stott, R. Stouffer, T. Sugiyama, R. Swart, D. Tirpak, C. Vogel, G. Yohe, R. Nottage, P. Madan, Climate Change 2007 Synthesis Report The Core Writing Team Rajendra K. Pachauri Andy Reisinger Synthesis Report Chairman Head, Technical Support Unit IPCC IPCC Synthesis Report, IPCC Core Writing Team Technical Support Unit for the Synthesis Report, 2007.

[8] Z. Jiang, T. Xiao, V.L. Kuznetsov, P.P. Edwards, Philos. Trans. A. Math. Phys. Eng. Sci. 368 (2010) 3343.

[9] K. KOLASINSKI, Curr. Opin. Solid State Mater. Sci. 10 (2006) 129.

[10] V.P. Indrakanti, J.D. Kubicki, H.H. Schobert, Energy Environ. Sci. 2 (2009) 745.

[11] G. Centi, S. Perathoner, Catal. Today 148 (2009) 191.

[12] L. Dong, Effects of Metal Modification on Titanium Dioxide for Photocatalytic Reduction of Carbon Dioxide, Nottinghim University, 2009.

[13] Xu, J. a Moulijn, Energy & Fuels 10 (1996) 305.

[14] C. Le Quéré, R.J. Andres, T. Boden, T. Conway, R. a. Houghton, J.I. House, G. Marland, G.P. Peters, G.R. van der Werf, a. Ahlström, R.M. Andrew, L. Bopp, J.G. Canadell, P. Ciais, S.C. Doney, C. Enright, P. Friedlingstein, C. Huntingford,

a. K. Jain, C. Jourdain, E. Kato, R.F. Keeling, K. Klein Goldewijk, S. Levis, P. Levy, M. Lomas, B. Poulter, M.R. Raupach, J. Schwinger, S. Sitch, B.D. Stocker, N. Viovy, S. Zaehle, N. Zeng, Earth Syst. Sci. Data 5 (2013) 165.

[15] D. US Energy Department, Carbon Cycling and Biosequestration, 2008.

[16] M.M. Metz, Bert Davidson, Ogunlade Coninck, Heleen de Loos, CARBON DIOXIDE CAPTURE, 2007.

[17] H. Herzog, D. Golomb, (2004) 1.

[18] B.M. Bhanage, M. Arai, Transformation and Utilization of Carbon Dioxide, Springer Berlin Heidelberg, Berlin, Heidelberg, 2014.

[19] E. V. Kondratenko, G. Mul, J. Baltrusaitis, G.O. Larrazábal, J. Pérez-Ramírez, Energy Environ. Sci. 6 (2013) 3112.

[20] W. Wang, S. Wang, X. Ma, J. Gong, Chem. Soc. Rev. 40 (2011) 3703.

[21] T. Abe, M. Tanizawa, K. Watanabe, A. Taguchi, Energy Environ. Sci. 2 (2009) 315.

[22] S. Sharma, Z. Hu, P. Zhang, E.W. McFarland, H. Metiu, J. Catal. 278 (2011) 297.

[23] J.-N. Park, E.W. McFarland, J. Catal. 266 (2009) 92.

[24] F. Ocampo, B. Louis, A.-C. Roger, Appl. Catal. A Gen. 369 (2009) 90.

[25] G. Du, S. Lim, Y. Yang, C. Wang, L. Pfefferle, G. Haller, J. Catal. 249 (2007) 370.

[26] Y. Hori, (2010) 1.

[27] Y. Hori, A. Murata, R. Takahashi, J. Chem. Soc. Faraday Trans. 1 Phys. Chem. Condens. Phases 85 (1989) 2309.

[28] Y. Hori, H. Wakebe, T. Tsukamoto, O. Koga, Electrochim. Acta 39 (1994) 1833.

[29] C.J.H. et al. M. N. Mahmood, D. Masheder, 17 (1987) 1223.

[30] M. Castellote, N. Bengtsson, (2011).

[31] J. Herrmann, Catal. Today 53 (1999) 115.

[32] K. Kočí, L. Obalová, Z. Lacný, Chem. Pap. 62 (2008) 1.

[33] N. Zhang, (2013).

[34] W.-N. Wang, Aerosol Air Qual. Res. (2014) 1.

[35] T. INOUE, A. FUJISHIMA, S. KONISHI, K. HONDA, Nature 277 (1979) 637.

[36] V.P. Indrakanti, J.D. Kubicki, H.H. Schobert, Energy Environ. Sci. 2 (2009) 745.

[37] P. Usubharatana, D. McMartin, Ind. … 45 (2006) 2558.

[38] M. HALMANN, Nature 275 (1978) 115.

[39] T. INOUE, A. FUJISHIMA, S. KONISHI, K. HONDA, Nature 277 (1979) 637.

[40] K.R. Thampi, J. Kiwi, M. Grätzel, Nature 327 (1987) 506.

[41] K. Hirano, K. Inoue, T. Yatsu, J. Photochem. Photobiol. A Chem. 64 (1992) 255.

[42] O. Ishitani|, C. Inoue, Y. Suzuki, T. Ibusuki, J. Photochem. Photobiol. A Chem. 72 (1993) 269.

[43] M. Anpo, H. Yamashita, Y. Ichihashi, S. Ehara, J. Electroanal. Chem. 396 (1995) 21.

[44] H. Yamashita, A. Shiga, S. Kawasaki, Y. Ichihashi, S. Ehara, M. Anpo, Energy Convers. Manag. 36 (1995) 617.

[45] F. Saladin, L. Forss, I. Kamber, J. Chem. Soc. Chem. Commun. (1995) 533.

[46] F. Saladin, I. Alxneit, J. Chem. Soc. Faraday Trans. 93 (1997) 4159.

[47] S. Kaneco, Y. Shimizu, K. Ohta, T. Mizuno, J. Photochem. Photobiol. A Chem. 115 (1998) 223.

[48] H. Yamashita, Y. Fujii, Y. Ichihashi, S.G. Zhang, K. Ikeue, D.R. Park, K. Koyano, T. Tatsumi, M. Anpo, Catal. Today 45 (1998) 221.

[49] M. Subrahmanyam, Appl. Catal. B Environ. 23 (1999) 169.

[50] K. Ikeue, H. Yamashita, M. Anpo, T. Takewaki, J. Phys. Chem. B 105 (2001) 8350.

[51] I.-H. Tseng, W.-C. Chang, J.C.S. Wu, Appl. Catal. B Environ. 37 (2002) 37.

[52] K. Ikeue, S. Nozaki, M. Ogawa, M. Anpo, Catal. Today 74 (2002) 241.

[53] G. Guan, T. Kida, A. Yoshida, Appl. Catal. B Environ. 41 (2003) 387.

[54] G.R. Dey, A.D. Belapurkar, K. Kishore, J. Photochem. Photobiol. A Chem. 163 (2004) 503.

[55] I.-H. Tseng, J.C.-S. Wu, Catal. Today 97 (2004) 113.

[56] I.-H. Tseng, J.C.. Wu, H.-Y. Chou, J. Catal. 221 (2004) 432.

[57] P. Pathak, M.J. Meziani, L. Castillo, Y.-P. Sun, Green Chem. 7 (2005) 667.

[58] Y. Ku, W.-H. Lee, W.-Y. Wang, J. Mol. Catal. A Chem. 212 (2004) 191.

[59] J.C.S. Wu, H.-M. Lin, C.-L. Lai, Appl. Catal. A Gen. 296 (2005) 194.

[60] N. SASIREKHA, S. BASHA, K. SHANTHI, Appl. Catal. B Environ. 62 (2006) 169.

[61] X.-H. Xia, Z.-J. Jia, Y. Yu, Y. Liang, Z. Wang, L.-L. Ma, Carbon N. Y. 45 (2007) 717.

[62] S. Liu, Z. Zhao, Z. Wang, Photochem. Photobiol. Sci. 6 (2007) 695.

[63] P.-W. Pan, Y.-W. Chen, Catal. Commun. 8 (2007) 1546.

[64] G. LI, S. CISTON, Z. SAPONJIC, L. CHEN, N. DIMITRIJEVIC, T. RAJH, K. GRAY, J. Catal. 253 (2008) 105.

[65] T.-V. Nguyen, J.C.S. Wu, Appl. Catal. A Gen. 335 (2008) 112.

[66] O.K. Varghese, M. Paulose, T.J. Latempa, C.A. Grimes, Nano Lett. 9 (2009) 731.

[67] H.-C. Yang, H.-Y. Lin, Y.-S. Chien, J.C.-S. Wu, H.-H. Wu, Catal. Letters 131 (2009) 381.

[68] Q.-H. Zhang, W.-D. Han, Y.-J. Hong, J.-G. Yu, Catal. Today 148 (2009) 335.

[69] Z.-Y. Wang, H.-C. Chou, J.C.S. Wu, D.P. Tsai, G. Mul, Appl. Catal. A Gen. 380 (2010) 172.

[70] K. Kočí, K. Matějů, L. Obalová, S. Krejčíková, Z. Lacný, D. Plachá, L. Čapek, A. Hospodková, O. Šolcová, Appl. Catal. B Environ. 96 (2010) 239.

[71] Y. Li, W.-N. Wang, Z. Zhan, M.-H. Woo, C.-Y. Wu, P. Biswas, Appl. Catal. B Environ. 100 (2010) 386.

[72] H. Tsuneoka, K. Teramura, T. Shishido, T. Tanaka, J. Phys. Chem. C 114 (2010) 8892.

[73] S.C. Yan, S.X. Ouyang, J. Gao, M. Yang, J.Y. Feng, X.X. Fan, L.J. Wan, Z.S. Li, J.H. Ye, Y. Zhou, Z.G. Zou, Angew. Chem. Int. Ed. Engl. 49 (2010) 6400.

[74] Q. Liu, Y. Zhou, Z. Tian, X. Chen, J. Gao, Z. Zou, J. Mater. Chem. 22 (2012) 2033.

[75] C. Wang, R.L. Thompson, J. Baltrus, C. Matranga, J. Phys. Chem. Lett. 1 (2010) 48.

[76] C.-C. Yang, J. Vernimmen, V. Meynen, P. Cool, G. Mul, J. Catal. 284 (2011) 1.

[77] K. Kočí, V. Matějka, P. Kovář, Z. Lacný, L. Obalová, Catal. Today 161 (2011) 105.

[78] P.-Q. Wang, Y. Bai, J.-Y. Liu, Z. Fan, Y.-Q. Hu, Catal. Commun. 29 (2012) 185.

[79] W.-H. Lee, C.-H. Liao, M.-F. Tsai, C.-W. Huang, J.C.S. Wu, Appl. Catal. B Environ. 132-133 (2013) 445.

[80] Y. Wang, B. Li, C. Zhang, L. Cui, S. Kang, X. Li, L. Zhou, Appl. Catal. B Environ. 130-131 (2013) 277.

[81] K.S.W. Sing, D.H. Everett, R. a. W. Haul, L. Moscou, R. a. Pierotti, J. Rouquérol, T. Siemieniewska, Pure Appl. Chem. 57 (1985) 603.

[82] M. Kruk, M. Jaroniec, Chem. Mater. 13 (2001) 3169.

[83] S. Brunauer, P.H. Emmett, E. Teller, J. Am. Chem. Soc. 60 (1938) 309.

[84] T. Ohno, K. Sarukawa, K. Tokieda, M. Matsumura, J. Catal. 203 (2001) 82.

[85] G. Tian, H. Fu, L. Jing, B. Xin, K. Pan, J. Phys. Chem. C 112 (2008) 3083.

[86] Z. Zhang, C.-C. Wang, R. Zakaria, J.Y. Ying, J. Phys. Chem. B 102 (1998) 10871.

[87] V.K. Pecharsky, P.Y. Zavalij, Fundamentals of Powder Diffraction and Structural Characterization of Materials, 2009.

[88] Y. Waseda, E. Matsubara, K. Shinoda, X-Ray Diffraction Crystallography, Springer-Verlag Berlin Heidelberg, 2011.

[89] J.M. Boone, X-Ray Production, Interaction, and Detection in Diagnostic Imaging, SPIE Press, Bellingham, 2000.

[90] B. Xin, L. Jing, Z. Ren, B. Wang, H. Fu, J. Phys. Chem. B 109 (2005) 2805.

[91] R. Sellappan, Mechanisms of Enhanced Activity of Model TiO2/Carbon and TiO2/Metal Nanocomposite Photocatalysts, Chalmers University of Technology Goteborg, Sweden, 2013.

[92] Z. Erlangung, M. Uyanik, Synthesis and Characterization of TiO 2 Nanostars, 2008.

[93] D. Shindo, T. Oikawa, Analytical Electron Microscopy for Materials Science, Springer Japan, Tokyo, 2003.

[94] B. Fultz, J.M. Howe, Transmission Electron Microscopy and Diffractometry of Materials, Springer Berlin Heidelberg, Berlin, Heidelberg, 2008.

[95] S.D. Sawant, a. a. Baravkar, R.N. Kale, Int. J. Pharma Bio Sci. 2 (2011) 513.

[96] L.E. Amand, C.J. Tullin, Dep. Energy Conversion, Chalmers Univ. Technol. Sweden (1999) 1.

[97] J.P. Redfern, Nature 173 (1954) 1011.

[98] Z. Aslam, R. a. Shawabkeh, I. a. Hussein, N. Al-Baghli, M. Eic, Appl. Surf. Sci. 327 (2015) 107.

[99] B. Gao, G.Z. Chen, G. Li Puma, Appl. Catal. B Environ. 89 (2009) 503.

[100] N. Riaz, M.A. Bustam, F.K. Chong, Z.B. Man, M.S. Khan, A.M. Shariff, 2014 (2014).

[101] L.S. Yoong, F.K. Chong, B.K. Dutta, Energy 34 (2009) 1652.

[102] M. a. Behnajady, H. Eskandarloo, Chem. Eng. J. 228 (2013) 1207.

[103] H. Zhang, H. Lu, Y. Zhu, F. Li, R. Duan, M. Zhang, X. Wang, Powder Technol. 227 (2012) 9.

[104] E.N. Alvar, M. Rezaei, H.N. Alvar, Powder Technol. 198 (2010) 275.

[105] D. Gao, Q. Wang, H. Qiao, Y. Cai, F. Huang, Q. Wei, (n.d.).

[106] H. Ninsonti, W. Chomkitichai, (n.d.).

[107] I. Ganesh, P.P. Kumar, I. Annapoorna, J.M. Sumliner, M. Ramakrishna, N.Y. Hebalkar, G. Padmanabham, G. Sundararajan, Appl. Surf. Sci. 293 (2014) 229.

[108] G. Vasapollo, G. Mele, R. Del Sole, I. Pio, J. Li, S.E. Mazzetto, Molecules 16 (2011) 5769.

[109] M. Mirghani, U.A. Al-Mubaiyedh, M.S. Nasser, R. Shawabkeh, Sep. Purif. Technol. 141 (2015) 285.

[110] A. Patri, T. Umbreit, J. Zheng, K. Nagashima, P. Goering, S. Francke-Carroll, E. Gordon, J. Weaver, T. Miller, N. Sadrieh, S. McNeil, M. Stratmeyer, J. Appl. Toxicol. 29 (2009) 662.

[111] C. X-rays, Uranium 100 (n.d.) 14001.

[112] S. Rengaraj, S. Venkataraj, J.W. Yeon, Y. Kim, X.Z. Li, G.K.H. Pang, Appl. Catal. B Environ. 77 (2007) 157.

[113] T.Theivasanthi, M.Alagar, arXiv (2013).

[114] K. Thamaphat, P. Limsuwan, B. Ngotawornchai, Nat. Sci. 42 (2008) 357.

[115] J. Gajendiran, V. Rajendran, Der Pharma Chem. 4 (2012) 1879.

[116] T. Theivasanthi, Arxiv Prepr. arXiv1003.6068 (2010).

[117] C.Y. Tsai, H.C. Hsi, T.H. Kuo, Y.M. Chang, J.H. Liou, Aerosol Air Qual. Res. 13 (2013) 639.

[118] A.S. Lanje, S.J. Sharma, R.B. Pode, R.S. Ningthoujam, Library (Lond). 1 (2010) 36.

[119] Y. Kobayashi, Y. Abe, T. Maeda, Y. Yasuda, T. Morita, J. Mater. Res. Technol. 3 (2014) 114.

[120] J.J. Lv, M.Y. Li, Q.X. Zeng, Adv. Mater. Res. 308-310 (2011) 715.

[121] S. Cho, J.-W. Jang, J.S. Lee, K.-H. Lee, Nanoscale 2 (2010) 2199.

[122] D. Rusu, G. Rusu, D. Luca, Acta Phys. Pol. A 119 (2011) 850.

[123] N.T. Mai, T.T. Thuy, D.M. Mott, S. Maenosono, CrystEngComm 15 (2013) 6606.

[124] Z. Zhong, S. Clouser, D. Vanek, 78 (2014) 1.

[125] S. Talam, S.R. Karumuri, N. Gunnam, ISRN Nanotechnol. 2012 (2012) 1.

[126] C.S. Prajapati, P.P. Sahay, Appl. Surf. Sci. 258 (2012) 2823.

[127] D. Wu, Y. Jiang, J. Liu, Y. Yuan, J. Wu, K. Jiang, D. Xue, Nanoscale Res. Lett. 5 (2010) 1779.

[128] V. Krishnakumar, K. Mohan Kumar, B.K. Mandal, F.-R.N. Khan, Sci. World J. 2012 (2012) 1.

[129] Z. Li, B. Hou, Y. Xu, D. Wu, Y. Sun, W. Hu, F. Deng, J. Solid State Chem. 178 (2005) 1395.

[130] X. Yan, J. He, D.G. Evans, Y. Zhu, X. Duan, J. Porous Mater. 11 (2004) 131.

[131] W.Z. Weng, M.S. Chen, Q.G. Yan, T.H. Wu, Z.S. Chao, Y.Y. Liao, H.L. Wan, Catal. Today 63 (2000) 317.

[132] O. Spectra, (2013).

[133] C.P. Schultz, H.H. Eysel, H.H. Mantsch, M. Jackson, J. Phys. Chem. 100 (1996) 6845.

[134] H. BEHRENS, A. STUKE, Glas. Sci. Technol. 76 (n.d.) 176.

[135] K.K. Pandey, J. Appl. Polym. Sci. 71 (1999) 1969.

[136] M.P. Contreras, R.Y. Avula, R.K. Singh, Food Bioprocess Technol. 3 (2009) 629.

[137] M. Bjørgen, K.-P. Lillerud, U. Olsbye, S. Bordiga, A. Zecchina, J. Phys. Chem. B 108 (2004) 7862.

[138] B. Xin, P. Wang, D. Ding, J. Liu, Z. Ren, H. Fu, Appl. Surf. Sci. 254 (2008) 2569.

[139] K. Song, J. Zhou, J. Bao, Y. Feng, J. Am. Ceram. Soc. 91 (2008) 1369.

[140] H. Yamashita, H. Nishiguchi, N. Kamada, Res. Chem. Intermed. 20 (1994) 815.

[141] L.-L. Tan, W.-J. Ong, S.-P. Chai, A.R. Mohamed, Appl. Catal. B Environ. 166-167 (2015) 251.

[142] Roth, Chemical Oxidation: Technology for the Nineties, Volume 6, CRC Press, 1997.

Vitae

Name	:Adeem Ghaffar Rana
Nationality	:Pakistani
Date of Birth	:3/23/1989
Email	:ranaadeem@hotmail.com
Address	:14-Ittefaq town Extension Mansoorah Lahore
Academic Background	King Fahd University of Petroleum and Minerals Session Jan 2013-May 2015 Institute of Chemical Engineering & Technology Session 2006-2010 University of the Punjab, Lahore

JOURNAL PUBLICATIONS

1. Ali Al-Matar, Waqar Ahmad, **Adeem Rana**, Reyad Shawabkeh, "Direct methanation of carbon dioxide: Thermodynamic analysis and Performance using $Cu/K/Al_2O_3$ based catalysts" submitted to " International Journal of Hydrogen Energy"
2. Reyad Shawabkeh, Ibnelwaleed Hussein, Waqar Ahmad, **Adeem Rana**, " Synthesis of new Cu-aluminosilicate catalyst for CO_2 capture and conversion to hydrocarbons", 4th International Gas Processing Symposium, October 26–27, 2014, Doha, Qatar (Book Chapter)
3. **Adeem Rana**, Ali Al-Matar, Waqar Ahmad, Reyad Shawabkeh, "Synthesis and characterization of of $Cu-Zn/TiO_2$ for the photocatalytic conversion of CO_2 " (Ready to submit)
4. Ali Al-Matar, Waqar Ahmad, **Adeem Rana**, Reyad Shawabkeh, "Characterization and catalytic performance of $Cu/K/Al_2O_3$ based catalysts for methanation of carbon dioxide " (Ready to submit)
5. Waqar Ahmad, Ali Al-Matar, **Adeem Rana**, Reyad Shawabkeh, "Kinetics study for methanation of carbon dioxide using $Cu/K/Al_2O_3$ based catalysts " (in progress)

CONFERENCE PAPERS

1. Reyad Shawabkeh*, Ali Al-Matar, Waqar Ahmad, **Adeem Rana**, "Synthesis and characterization of new Cu-based catalyst for conversion of CO_2", 7th international workshop characterization of porous material from Angstroms to millimeters, May 3-6, 2015, Florida, USA.

PROJECTS AND REPORTS

- Plant design project on ***210 MW Natural Gas Fired Combined Cycle Steam Power Plant***
- Research project on ***Extraction of Rare Earth Metals from Carbonatite Rock using Liquid- Liquid Extraction***

WORK EXPERIENCE

- Worked in **Style Textile Pvt(Ltd)** as **Assistant Manager** in **Processing** from May 2010 to February 2013
    - **Major Responsibilities**
        - Planning and Execution according to machines
        - To meet all testing Parameters set By the Buyers Like **"NIKE"**,**"REEBOK"**,**"ADIDAS"** and **"HURLEY"** etc
        - Implementation of **ERP**
- 4 weeks internship at ***ICI Polyester Fibre***, Pakistan

RESEARCH EXPERIENCE

Experience of the operation, calibration and interpretation of results of

- Gas Chromatograph & Mass Spectrometer (GC/MS)
- X-Ray Diffraction (XRD)
- Scanning Electron Microscope / Energy-dispersive X-ray spectroscopy (SEM/EDX)
- Thermo Gravimetric Analysis (TGA)
- Fourier transform infrared spectroscopy (FTIR)
- Brunauer–Emmett–Teller (BET)

COMPUTER SKILLS

- HYSYS
- Matlab
- Mathematica
- Microsoft Office (Excel, Word and Power Point)
- Auto CAD
- Origin

ACHIEVEMENTS

- Saudi government scholarship for MS chemical engineering at KFUPM
- Got the merit scholarship in the 1st year of chemical engineering from ICET
- Participated in One day symposium on engineering sciences at ICET in April 2009